Supplementary Material for 'Thermally activated sliding in ice sheet flow. Part 2: The stability of subtemperate regions'

Elisa Mantelli[1,2,*] and Christian Schoof[2]

[1]Geophysics Department, Stanford University, Stanford (CA), USA
[2]Department of Earth, Ocean and Atmospheric Sciences, University of British Columbia, Vancouver, CA
[*]present address: AOS Program, Princeton University, Princeton (NJ), USA

September 20, 2019

Contents

1 The ice sheet scale model with boundary conditions as in Fowler 2001 **2**
1.1 An ice sheet model with subtemperate sliding 2
1.2 Stability of the subtemperate region 4
1.3 Stability of the subtemperate-temperate boundary 6

2 Asymptotically reduced models for a subtemperate ice slab **9**
2.1 Master model 9
2.2 An ice thickness scale model with $\delta = 0$ 11
2.3 The distinguished limit $\delta \sim \varepsilon^{1/2}$ 13

3 Stability of the ice thickness scale problem with $\delta = 0$ **17**
3.1 Model reformulation 17
3.2 An intermediate time scale, $t \sim \varepsilon^{-1}$ 18
3.3 A fast time scale, $t \sim \varepsilon^{-2}$ 20

4 Stability of the ice thickness scale problem with $\delta \sim \varepsilon^{1/2}$ **22**
4.1 Stability analysis 22
4.2 Approximation 27
4.3 A non-linear model in the short wavelength limit, $k_n \to +\infty$ 33

5 Stability at longer length scales with $\delta \sim \varepsilon^{1/2}$ **38**
5.1 Stability of the intermediate scale model 38
5.2 Stability of the ice sheet scale model 42

6 The discrete ice thickness scale subtemperate slab with $\delta \sim \varepsilon^{1/2}$ 43
6.1 Model reformulation 43
6.2 Discretization 44

A Supplementary Figures 48

1 The ice sheet scale model with boundary conditions as in Fowler 2001

1.1 An ice sheet model with subtemperate sliding

We start our analysis by re-stating the ice sheet scale model with subtemperate sliding that we derived in the companion paper (§5(a)). Let us consider a laterally uniform ice sheet with surface elevation $z = s(x,t)$ and bed elevation $z = b(x)$, where $z = 0$ denotes sea level. Here x is the horizontal spatial coordinate, scaled with the length of the ice sheet, z is the vertical coordinate, and t is time scaled with the natural advective time scale of the ice sheet. The ice has thickness $h(x,t) = s - b$, and extends from a divide located at $x = 0$ to a margin located at $x = x_g$. The velocity field scaled with the shear velocity is $\boldsymbol{u} = (u, w)$, while T is temperature, scaled with the difference between the melting point and a representative surface temperature. At this large horizontal length scale, it is justified to take the limit of small ice sheet aspect ratio, $\varepsilon \to 0$ [that is, the so called shallow ice approximation, 1, 2], leading to a horizontal velocity u and basal shear stress τ_b

$$u = \frac{1}{2}\left[h^2 - (s-z)^2\right]\left|\frac{\partial s}{\partial x}\right| + u_b, \quad \tau_b = h\left|\frac{\partial s}{\partial x}\right|, \tag{1a}$$

where $u_b = u(z = b)$ is the sliding velocity, which for now we regard simply as a function of basal shear stress and basal temperature. From the expression above we compute the mass flux as

$$q = \int_b^s u \, \mathrm{d}z = \frac{h^2}{3}\tau_b + u_b h; \tag{1b}$$

then, along-flow changes in q drive the evolution of the ice surface through the diffusion equation

$$\frac{\partial s}{\partial t} + \frac{\partial q}{\partial x} = \dot{b}, \tag{1c}$$

where $\dot{b}$ describes mass gain by surface accumulation (if positive) or loss by melt or sublimation (if negative). Boundary conditions for eq. (1c) at the divide and grounding line are

$$q = 0 \quad \text{on} \quad x = 0, \quad h = -\rho_w \rho^{-1} b \quad \text{on} \quad x = x_g, \quad q = Q_g(h) \quad \text{on} \quad x = x_g, \tag{1d}$$

whereby we have assumed that the ice sheet is symmetric at $x = 0$, and that it has a marine margin whose location is defined by incipient flotation, eq. ($1d_2$), and by a flux condition, eq. ($1d_3$), where ρ, ρ_w denote ice and water density, respectively, and the function Q_g is given by Schoof [3].

The vertical velocity w decouples from the leading order mechanical problem and is the solution to the local mass conservation

$$\frac{\partial u}{\partial x} + \frac{\partial w}{\partial z} = 0 \quad \text{on} \quad b < z < s, \tag{2a}$$

which can be integrated between the bed and the ice surface straightforwardly to compute w using $(1a_1)$ for the horizontal velocity u along with the basal boundary condition

$$u_b \frac{\partial b}{\partial x} - w = 0 \quad \text{on} \quad z = b. \tag{2b}$$

Lastly, omitting terms of order $O(\varepsilon^2)$, the leading order heat transport problem reads

$$Pe \left(\frac{\partial T}{\partial t} + u \frac{\partial T}{\partial x} + w \frac{\partial T}{\partial z} \right) - \frac{\partial^2 T}{\partial z^2} = \alpha a(x, z, t) \qquad \text{for} \quad b < z < s, \tag{3a}$$

$$Pe \frac{\partial T}{\partial t} - \frac{\partial^2 T}{\partial z^2} = 0 \qquad \text{for} \quad z < b, \tag{3b}$$

with strain heating $a = (\partial u / \partial z)^2$. In the latter equations, Pe is the ice sheet scale Péclet number, which can be seen as the ratio of the divergences of advective and diffusive heat fluxes, where the latter is dominated by vertical diffusion at the ice sheet scale. The parameter α denotes instead the strength of strain heating compared to the background conductive heat flux in the ice. We regard both parameters as strictly $O(1)$.

Boundary conditions for the heat transport problem at the surface and in the far field of the bed are

$$T = -T_s \qquad \text{on} \quad z = s, \tag{3c}$$

$$-\frac{\partial T}{\partial z} \to \nu \qquad \text{as} \quad z \to -\infty. \tag{3d}$$

In order to specify boundary conditions at the bed, $z = b$, it is useful to first examine the physics of basal sliding, which we assume to be thermally controlled. In general, temperature-dependent sliding is modelled through an explicitly temperature-dependent sliding law of the form [4, 5]

$$u_b = \gamma^{-1} F(T/\delta) \tau_b, \tag{3e}$$

where $\gamma \sim O(1)$ is a non-dimensional friction coefficient, while $\delta \ll 1$ is a positive parameter that compares the range of temperatures below the melting point over which subtemperate sliding is $O(1)$ to the typical temperature scale of the ice sheet. The dependence of sliding on temperature is described by the function F, which is is monotonically increasing in T subject to the constraint that $T \leq 0$ (where $T = 0$ is the melting point), and such that $F(0) = 1$. The fully temperate sliding law is recovered when the bed attains the melting point, while significant sliding occurs within a temperature range of δbelow the melting point, so $F(T/\delta) \approx 0$ when $|T| \ll \delta$.

Taking the limit $\delta \to 0$ allowed us to simplify basal boundary conditions (on $z = b$) for the ice sheet scale model to (see §5(c) of the companion paper for an asymptotic justification)

$$\left[\frac{\partial T}{\partial z} \right]_-^+ = [T]_-^+ = u_b = 0 \qquad \text{if} \quad T < 0, \tag{3f}$$

$$\left[\frac{\partial T}{\partial z} \right]_-^+ + \alpha u_b \tau_b = T = 0 \qquad \text{if} \quad u_b < \gamma^{-1} \tau_b, \tag{3g}$$

$$T = u_b - \gamma^{-1} \tau_b = 0 \qquad \text{if} \quad m > 0, \tag{3h}$$

with the basal melt rate m defined as

$$m = \left[\frac{\partial T}{\partial z} \right]_-^+ + \alpha \tau_b u_b \quad \text{on} \quad z = b, \tag{3i}$$

and $[g(z_0)]^+_- = g(z \to z_0^+) - g(z \to z_0^-)$. Note that boundary conditions (3f-3h), previously proposed by Fowler [6], implicitly identify three distinct regions of the ice sheet: a cold-based region, where bed temperature is well below the melting point and no sliding occurs; a subtemperate region, where bed temperature is approximately the melting point and $O(1)$ sliding occurs subject to the constraint that the ice-bed contact remains in thermal balance; a temperate-based region where the basal melt rate remains positive and fully temperate sliding occurs. We denote the cold-subtemperate and subtemperate-temperate boundaries as $x = x_s$ and $x = x_t$, respectively, and we demand that at these boundaries the boundary conditions (3f), (3g), and (3g), (3h) hold simultaneously, leading to

$$T(z=b) = u_b = 0 \quad \text{at} \quad x = x_s, \quad \gamma^{-1}\tau_b = -\left[\frac{\partial T}{\partial z}\right]^+_- (\alpha\tau_b)^{-1},\ m = 0 \quad \text{at} \quad x = x_t, \tag{3j}$$

which fix the location of subdomain boundaries. Lastly, continuity of mass and temperature is ensured demanding

$$[q]^+_- = [h]^+_- = \left[\frac{\partial T}{\partial z}\right]^+_- = 0 \quad \text{on} \quad x = x_s, x_t. \tag{3k}$$

1.2 Stability of the subtemperate region

1.2.1 A shallow subtemperate slab

Let us consider the ice sheet scale model of §1.1, and restrict ourselves to the subtemperate region. We then take the limit of a short horizontal length scale within the shallow ice approximation, which yields the slab model

$$\frac{\partial s}{\partial t} + \frac{\partial q}{\partial x} = 0, \tag{4a}$$

with mass flux (1b), and sliding velocity u_b defined by the basal energy budget

$$-Q + \nu + \alpha\tau_b u_b = 0, \tag{4b}$$

where $Q = -\partial T/\partial z|_{z\to b^+}$, and τ_b is given by eq. (1a$_2$). Note that, as basal temperature is approximately at the melting point in the subtemperate region, the heat equation in the bed (3b) can be integrated analytically, leading to $-\partial T/\partial z = \nu$ for $z < b$; this justifies the form of the basal heat flux in the bed in eq. (4b). Regarding the heat equation in the ice, it is important to note that at this shorter horizontal length scale the local Péclet number Pe_{slab} is large. As basal temperature is at the melting point in the subtemperate region, then the thermal model for the ice reduces to the $Q-$equation (see §3(b) of the companion paper)

$$\frac{\partial Q}{\partial t} + u_b\frac{\partial Q}{\partial x} - Q\frac{\partial u_b}{\partial x} = 0, \tag{4c}$$

which completes our slab model.

1.2.2 Linearization

We are interested in the fate of short-wavelength perturbations about the steady state of the subtemperate ice slab described by eqs. (4). As usual, we linearize model variables around their steady state (denoted with $\bar{\cdot}$) as

$$h = \bar{h}+\beta h', \quad u_b = \bar{u}_b+\beta u_b', \quad \tau_b = \bar{\tau}_b+\beta\tau_b', \quad \frac{\partial s}{\partial x} = \frac{\mathrm{d}\bar{s}}{\mathrm{d}x}+\beta\frac{\partial h'}{\partial x}, \quad Q = \bar{Q}+\beta Q', \quad \text{with } \beta \ll 1, \tag{5}$$

where surface slope $\mathrm{d}\bar{s}/\mathrm{d}x = \mathrm{d}b/\mathrm{d}x$ is constant, and $\bar{h}, \bar{u}_b, \bar{Q}$ do not depend on x. Upon linearization, to order $O(\beta)$ we have

$$\frac{\partial h'}{\partial t} + \frac{\partial}{\partial x}\left[\frac{\bar{h}^2}{3}\tau_b' + \frac{2\bar{h}\bar{\tau}_b}{3}h' + \bar{u}_b h' + \bar{h}u_b'\right] = 0, \tag{6a}$$

$$\frac{\partial Q'}{\partial t} + \bar{u}_b\frac{\partial Q'}{\partial x} - \bar{Q}\frac{\partial u_b'}{\partial x} = 0, \tag{6b}$$

with basal energy budget

$$Q' + \alpha\left(\bar{\tau}_b u_b' + \bar{u}\tau_b'\right) = 0, \tag{6c}$$

and perturbed basal shear stress

$$\tau_b' = -\bar{h}\frac{\partial h'}{\partial x} - \frac{\mathrm{d}\bar{s}}{\mathrm{d}x}h'. \tag{6d}$$

1.2.3 Stability analysis, $\sigma \sim k^2$

We now seek an approximation to the solution of the linear system above that holds for short wavelength perturbations. For simplicity, assume that the domain is periodic in x with period $L \sim O(1)$. A solution to the linearized model can then be found assuming separation of variables, and using a Fourier series in x. We define

$$f_n(t) = \frac{1}{L}\int_0^L f'(x,t)\exp\left(-ik_n x\right)\mathrm{d}x, \quad k_n = \frac{2\pi n}{L}, \tag{7}$$

with $f_n = \hat{f}_n\exp\left(\sigma t\right)$, and $\sigma \in \mathbb{C}$. To find a solution in the limit $k_n \to \infty$, we apply the rescalings

$$\hat{h}_n = k_n^{-2}\tilde{h}_n, \quad \hat{u}_{b,n} = k_n^{-1}\tilde{u}_{b,n}, \quad \hat{\tau}_{b,n} = k_n^{-1}\tilde{\tau}_{b,n}, \quad \hat{Q}_n = k_n^{-2}\tilde{Q}_n, \quad \sigma = k_n^2\tilde{\sigma}, \tag{8}$$

and expand as $\tilde{f}_n = \tilde{f}_n^{(0)} + O(k_n^{-1})$. Omitting terms of order $O(k_n^{-1})$, we find the following algebraic leading order problem

$$\tilde{\sigma}^{(0)}\tilde{h}_n^{(0)} + \frac{\bar{h}^3}{3}\tilde{h}_n^{(0)} + i\bar{h}\tilde{u}_{b,n}^{(0)} = 0, \tag{9a}$$

$$\tilde{\sigma}^{(0)}\tilde{Q}_n^{(0)} - i\bar{Q}\tilde{u}_{b,n}^{(0)} = 0, \tag{9b}$$

$$\bar{\tau}_b\tilde{u}_{b,n}^{(0)} + \bar{u}_b\tilde{\tau}_{b,n}^{(0)} = 0, \tag{9c}$$

$$\tilde{\tau}_{b,n}^{(0)} = -i\bar{h}\tilde{h}_n^{(0)} \tag{9d}$$

The solution to the perturbed problem above reads

$$\tilde{\sigma}^{(0)} = \frac{\bar{h}}{\bar{\tau}_b}\left(-\frac{\bar{\tau}_b\bar{h}^2}{3} + \bar{u}_b\bar{h}\right), \quad \tilde{u}_{b,n}^{(0)} = i\frac{\bar{u}_0\bar{h}_0}{\bar{\tau}_b}\tilde{h}_n^{(0)}, \quad \tilde{Q}_n^{(0)} = i\frac{\bar{Q}}{\tilde{\sigma}^{(0)}}\tilde{u}_{b,n}^{(0)}. \tag{9e}$$

$\tilde{\sigma}^{(0)}$ is purely real, hence the its sign determines the growth or decay of perturbations. The sign of $\tilde{\sigma}^{(0)}$ is dictated by the term in brackets in ($9e_1$): recalling the definition of the mass flux (1b), we understand that these terms represent the difference between the mass flux by sliding and the mass flux by shearing. When sliding is larger than shearing (*fast sliding*) the system is unstable, while it is stable in the opposite case (*slow sliding*). Given that $\sigma \sim k_n^2$, we conclude that the fast sliding regime is ill-posed due to backward diffusion.

1.2.4 Stability analysis, $\sigma \sim k$

The analysis above identifies the slow sliding regime as stable. We are now going to show that another dominant balance is possible in the shortwavelength limit, and that this leads to an instability with $\sim O(1)$ growth rate in the slow sliding regime.

By replacing the rescalings (8) with

$$\hat{h}_n = k_n^{-2}\tilde{h}_n, \quad \hat{u}_{b,n} = k_n^{-1}\tilde{u}_{b,n}, \quad \hat{\tau}_{b,n} = k_n^{-1}\tilde{\tau}_{b,n}, \quad \hat{Q}_n = k_n^{-1}\tilde{Q}_n, \quad \sigma = k_n\tilde{\sigma}, \tag{10}$$

and following the same approach outlined for the $\sigma \sim k_n^2$ mode, we find the leading order problem

$$\frac{\bar{h}^3}{3}\tilde{h}_n^{(0)} + i\bar{h}\tilde{u}_{b,n}^{(0)} = 0, \tag{11a}$$

$$\tilde{\sigma}^{(0)}\tilde{Q}_n^{(0)} + i\bar{u}\tilde{Q}_n^{(0)} - i\bar{Q}\tilde{u}_{b,n}^{(0)} = 0, \tag{11b}$$

$$\tilde{Q}_n^{(0)} + \alpha\left(\bar{\tau}_b\tilde{u}_{b,n}^{(0)} + \bar{u}_b\tilde{\tau}_{b,n}^{(0)}\right) = 0, \tag{11c}$$

$$\tilde{\tau}_{b,n}^{(0)} = -i\bar{h}\tilde{h}_n^{(0)}. \tag{11d}$$

The solution to this problem is a travelling wave,

$$\tilde{\sigma}^{(0)} = -\frac{i\bar{h}(3\alpha\bar{u}_b^2 + \bar{h}\nu)}{3\alpha\left(-\frac{\bar{\tau}_b\bar{h}^2}{3} + \bar{u}_b\bar{h}\right)}, \quad \tilde{u}_{b,n}^{(0)} = \frac{i\bar{h}^2}{3}\tilde{h}_n^{(0)}, \quad \tilde{Q}_n^{(0)} = -i\alpha\left(-\frac{\bar{\tau}_b\bar{h}^2}{3} + \bar{u}_b\bar{h}\right)\tilde{h}_n^{(0)}, \tag{11e}$$

where the relative importance of sliding compared to shearing determines whether the wave propagates upstream or downtream. Growth is determined by the $O(k_n^{-1})$ problem, which reads

$$\tilde{h}_n^{(0)}\tilde{\sigma}^{(0)} + \frac{\bar{h}^3}{3}\tilde{h}_n^{(1)} + i\bar{h}\bar{\tau}_b\tilde{h}_n^{(0)} + i\bar{h}\tilde{u}_{b,n}^{(1)} + i\bar{u}_b\tilde{h}_n^{(0)} = 0, \tag{11f}$$

$$\tilde{\sigma}^{(1)}\tilde{Q}_n^{(0)} + \tilde{\sigma}^{(0)}\tilde{Q}_n^{(1)} + i\bar{u}\tilde{Q}_n^{(1)} - i\bar{Q}\tilde{u}_{b,n}^{(1)} = 0, \tag{11g}$$

$$\tilde{Q}_n^{(1)} + \alpha\left(\bar{\tau}_b\tilde{u}_{b,n}^{(1)} + \bar{u}_b\tilde{\tau}_{b,n}^{(1)}\right) = 0, \tag{11h}$$

$$\tilde{\tau}_{b,n}^{(1)} = -i\bar{h}\tilde{h}_n^{(1)} + \left|\frac{\mathrm{d}\bar{s}}{\mathrm{d}\bar{x}}\right|\tilde{h}_n^{(0)}. \tag{11i}$$

The first order correction to the eigenvalue is purely real, and reads

$$\tilde{\sigma}^{(1)} = \frac{\bar{u}_b\bar{\tau}_b\bar{Q}\bar{h}\left[\left(\frac{\bar{\tau}_b\bar{h}^2}{3} - \bar{u}_b\bar{h}\right) + \frac{\bar{h}}{3\alpha\bar{\tau}_b}\left(\alpha\bar{h}\bar{\tau}_b + 3\nu\right)\right]}{3\alpha\left(\frac{\bar{\tau}_b\bar{h}^2}{3} - \bar{u}_b\bar{h}\right)^3}. \tag{11j}$$

For slow sliding $\bar{\tau}_b\bar{h}^2/3 > \bar{u}_b\bar{h}$, thus $\tilde{\sigma}^{(1)} > 0$. We therefore conclude that also in the slow sliding regime a shallow ice slab with subtemperate sliding is unstable to short wavelength perturbations, although the growth rate of these perturbations does not depend on their wavelength.

1.3 Stability of the subtemperate-temperate boundary

We now consider the boundary between subtemperate and temperate region located at $x = x_t$. Like in §2.1, we are concerned with the fate of short wavelength perturbations, thus restrict ourselves to a shallow ice slab in the vicinity of $x = x_t$.

1.3.1 Rescalings and linearization

Let us consider the slab model (4), along with the fully temperate sliding law ($3h_2$) and the continuity statements ($3j_2$) and (3k), and rescale variables as

$$x^* = k(x - x_t), \quad t^* = kt, \quad z^* = z, \quad Q^* = Q, \quad u_b^* = u_b, \quad h^* = h, \quad \tau_b^* = \tau_b, \tag{12a}$$

where $k^{-1} \ll 1$ is a short horizontal scale. In addition, we expand dependent variables about their steady state (denoted by $\bar{\cdot}$, and such that steady state variables to leading order depend only on the unscaled coordinate x) as

$$h^* = \bar{h}^* + \beta k^{-2}\tilde{h}, \quad Q^* = \bar{Q}^* + \beta k^{-1}\tilde{Q}, \quad u_b^* = \bar{u_b}^* + \beta k^{-1}\tilde{u}_b, \quad \tau_b^* = \bar{\tau_b}^* + \beta k^{-1}\tau_b, \quad x_t^* = \beta k^{-1}x_t', \quad \beta \ll 1, \tag{12b}$$

where x_t' is a perturbation of the subtemperate-temperate boundary, and steady state variables are of the form

$$\bar{f}^* = \bar{f}|_{x=x_t} + k^{-1}\left.\frac{\mathrm{d}\bar{f}}{\mathrm{d}x}\right|_{x=x_t} x^* + O(k^{-2}). \tag{12c}$$

Lastly, we assume that perturbations are separable, so $f' = \tilde{f}\exp(\sigma t^*)$, with σ to be determined. Equipped with these transformations, the linearized, $O(\beta)$ problem reads

$$\frac{\mathrm{d}}{\mathrm{d}x^*}\left[-\frac{1}{3}\bar{h}^3\frac{\mathrm{d}\tilde{h}}{\mathrm{d}x^*} + \bar{h}\tilde{u}_b\right] = 0, \tag{13a}$$

$$\sigma\tilde{Q} + \bar{u}\frac{\mathrm{d}\tilde{Q}}{\mathrm{d}x^*} - \bar{Q}\frac{\mathrm{d}\tilde{u}_b}{\mathrm{d}x^*} = 0, \tag{13b}$$

with the sliding velocity given by

$$-\tilde{Q} + \alpha\left(\bar{\tau}_b\tilde{u}_b - \bar{u_b}\bar{h}\frac{\mathrm{d}\tilde{h}}{\mathrm{d}x^*}\right) = 0 \qquad \text{for } x^* < 0, \tag{13c}$$

$$\tilde{u}_b = -\frac{\bar{h}}{\gamma}\frac{\mathrm{d}\tilde{h}}{\mathrm{d}x^*} \qquad \text{for } x^* > 0. \tag{13d}$$

Expanding about the subtemperate-temperate boundary, the continuity statements ($3j_2$) and (3k) become

$$\left[\tilde{h}\right]_-^+ = 0, \tag{13e}$$

$$-\frac{1}{3}\bar{h}^3\left[\frac{\mathrm{d}\tilde{h}}{\mathrm{d}x}\right]_-^+ + \bar{h}\left[\tilde{u}_b\right]_-^+ = 0, \tag{13f}$$

$$\left[\tilde{u}_b\right]_-^+ + \left[\frac{\mathrm{d}\bar{u}_b}{\mathrm{d}x}\right]_-^+ x_t' = 0, \tag{13g}$$

$$\left[\tilde{Q}\right]_-^+ + \left[\frac{\mathrm{d}\bar{Q}}{\mathrm{d}x}\right]_-^+ x_t' = 0, \tag{13h}$$

where we have omitted the subscript $|_{x=x_t}$ from steady state variables, and we have also used continuity of the steady state surface slope at the transition point to obtain (13e). Lastly, since we are seeking solutions with structure localized near the boundary, we demand that the eigenfunctions remain bounded for $x^* \to \pm\infty$.

1.3.2 Solution

We start by recognizing that mass conservation, eq. (13a), can be integrated directly and yields a relation between the perturbed sliding velocity $\tilde{u}_b$ and the perturbed surface slope, $\mathrm{d}\tilde{h}/\mathrm{d}x^*$. On the temperate side, $x^* > 0$, the sliding law (13d) gives $\tilde{u}_b$ as a function of $\mathrm{d}\tilde{h}/\mathrm{d}x^*$; thus substituting the sliding law into the integrated form of mass conservation we find

$$-\left(\frac{1}{3}\bar{h}^3 + \frac{\bar{h}^2}{\gamma}\right)\frac{\mathrm{d}\tilde{h}}{\mathrm{d}x^*} = C_h \quad \text{on } x^* > 0, \tag{14a}$$

with C_h an integration constant which we set to zero to ensure that $\tilde{h}$ remains bounded as $x^* \to +\infty$. It is then straightforward to obtain the solution for $\tilde{h}, \tilde{u}_b, \tilde{Q}$ on the temperate side,

$$\tilde{h} = H_+, \quad \tilde{u}_b = 0, \quad \tilde{Q} = Q_+ \exp\left\{-\frac{\sigma}{\bar{u}_b}x^*\right\} \quad \text{on } x^* > 0, \tag{14b}$$

where Q_+ is a constant to be determined, while we set $H_+ = 0$ without loss of generality. From ($14\mathrm{b}_3$) we note immediately that a bounded $\tilde{Q}$ demands $\mathrm{Re}[\sigma^{(0)}] > 0$; it then follows that, if a localized solution exists, it has to be unstable.

Next we move to the subtemperate side: here more algebra is required because mass and energy conservation are coupled through the sliding law. Using the solution on the temperate side (14b), and flux continuity across the boundary (13f), mass conservation gives

$$-\frac{1}{3}\bar{h}^3\frac{\mathrm{d}\tilde{h}}{\mathrm{d}x^*} + \bar{h}\tilde{u}_b = 0 \quad \text{for } x^* < 0 \tag{15a}$$

By combining the latter expression with the subtemperate sliding law (13c), we obtain a relation between sliding velocity and basal heat flux on the subtemperate side,

$$\tilde{u}_b = -\frac{\bar{h}^2}{3\alpha\left(\bar{h}^2\bar{\tau}_b - \bar{h}\bar{u}_b\right)}\tilde{Q} \quad \text{for } x^* < 0, \tag{15b}$$

where we recall that the term in brackets at the denominator is the difference between mass flux by shearing and mass flux by sliding. Equipped with the relation (15b), we can integrate energy conservation on the subtemperate side, which yields

$$\tilde{Q} = Q_- \exp\left\{-\left[\bar{u}_b - \frac{\bar{Q}\left(\bar{h}\right)^2}{3\alpha\left(\bar{h}^2\bar{\tau}_b - \bar{h}\bar{u}_b\right)}\right]^{-1}\sigma x^*\right\} \quad \text{for } x^* < 0. \tag{15c}$$

Lastly, substituting (15c) back into (15b), and then into the integrated mass conservation (15a), allows us to solve for $\tilde{h}$. We find

$$\tilde{h} = -\left[\bar{u}_b - \frac{\bar{Q}\bar{h}^2}{3\alpha\left(\bar{h}^2\bar{\tau}_b - \bar{h}\bar{u}_b\right)}\right]\frac{\tilde{Q}}{\sigma} + H_- \quad \text{for } x^* < 0, \tag{15d}$$

with H_-, Q_- integration constants to be determined.

At this stage, the only constraints yet to be satisfied are ice thickness, sliding velocity, and basal heat flux continuity at the transition point, eqs. (13e, 13g, 13h). We will now use them to find expressions for Q_-, Q_+, and σ as a function of x_t' and H_-. We start from continuity of the sliding

velocity, eq. (13g). Using the relationship between $\tilde{u}_b$ and $\tilde{Q}$ in the subtemperate region, eq. (15b), we find a relation between Q_- and x_t'

$$Q_- = -\frac{3\alpha\left[\bar{h}^2\bar{\tau}_b - \bar{h}\bar{u}_b\right]}{\bar{h}^2}\left[\frac{\mathrm{d}\bar{u}_b}{\mathrm{d}x}\right]_-^+ x_t', \tag{16a}$$

whereas continuity of the basal heat flux, eq. (13h), relates Q_+ to x_t',

$$Q_+ = -\left[\frac{\mathrm{d}\bar{Q}}{\mathrm{d}x}\right]_-^+ x_t' + Q_-. \tag{16b}$$

Finally, continuity of ice thickness, eq. (13e), yields an expression for the eigenvalue as a function of H_- and Q_-,

$$\sigma = \left[\bar{u}_b - \frac{\bar{Q}\bar{h}^2}{3\alpha\left(\bar{h}^2\bar{\tau}_b - \bar{h}\bar{u}_b\right)}\right]\frac{Q_-}{H_-}. \tag{16c}$$

It is clear from the expressions (16a-16c) that, for a given amplitude of the perturbation of the boundary x_t' and far field ice thickness H_-, the sign of the real part of the eigenvalue depends on the sign of the term in brackets in eq. (16c) and on the jump of the derivative of sliding velocity across the boundary. As for the latter, we showed in the supplementary materials for part I (§4.4) that $\left[\frac{\mathrm{d}\bar{u}_b}{\mathrm{d}x}\right]_-^+ < 0$; here we consider instead the term in brackets in eq. (16c), and the related issue of boundedness of the eigenfunctions in the far field.

As far as boundedness is concerned, the solution on the temperate side demands $\mathrm{Re}[\tilde{\sigma}^{(0)}] > 0$ through eq. (14b). Therefore the subtemperate eigenfunctions (15c, 15d) remain bounded provided

$$\bar{u}_b - \frac{\bar{Q}\bar{h}^2}{3\alpha\left(\bar{h}\bar{\tau}_b - \bar{h}\bar{u}_b\right)} < 0, \tag{16d}$$

which, for slow sliding ($\bar{h}^2\bar{\tau}_b - \bar{h}\bar{u}_b > 0$), can be satisfied only if

$$3\left(1 - \frac{\nu}{\bar{Q}}\right)\left(1 - \frac{1}{\gamma\bar{h}}\right) < 1, \quad \text{with} \quad \left(1 - \frac{1}{\gamma\bar{h}}\right) > 0, \tag{16e}$$

while no bounded solution is available for fast sliding. Going back to the eigenvalue, satisfying the inequalities above implies that the term in brackets in (16c) is negative, and that $\mathrm{sign}(\mathrm{Re}[Q_-]) = \mathrm{sign}(\mathrm{Re}[x_t'])$. To satisfy $\mathrm{Re}[\sigma^{(0)}] > 0$ we therefore demand that

$$\mathrm{sign}(\mathrm{Re}[x_t']) = \mathrm{sign}(\mathrm{Re}[H_-]), \tag{16f}$$

which is permissible because both x_t' and H_- are free parameters.

In summary, our analysis confirms that in the slow sliding regime small amplitude perturbations of the subtemperate-temperate boundary lead to localized perturbations of ice thickness, basal heat flux, and sliding velocity. We find that these perturbations are unstable, with their growth rate increasing as the wavelength decreases, thus this type of boundary is not viable.

2 Asymptotically reduced models for a subtemperate ice slab

2.1 Master model

We consider the Stokes problem for an ice slab with temperature-dependent sliding. The coordinate system is aligned with the bed, which we assume to be locally flat over the horizontal scales of interest

and tilted of an angle μ to the horizontal; so the $x-$ axis is parallel to the bed and pointing downslope, while the $z-$axis is perpendicular to the bed and pointing upwards. The ice-bed interface is located at $z = b$, and the ice surface at $z = s(x, t)$; $h(x, t) = s - b$ is the ice thickness, $\boldsymbol{u} = (u, w)$ is the velocity field, p is pressure, and T is temperature.

We introduce non-dimensional variables denoted with *, which relate to the dimensional ones through the rescalings $(x^*, z^*) = x/[x]$, $z^* = z/[z]$, etc. We consider scales for the ice sheet length $[x] = L$, surface accumulation $[\dot{b}]$, and temperature $[T] = T_{surf} - T_m$ as known quantities, and introduce the usual, shallow ice scale relationships [1, 2]

$$[w] = [\dot{b}], \quad [u] = [w]\varepsilon^{-1}, \quad [t] = [x][u]^{-1}, \quad [p] = \rho g[z]\cos(\mu), \quad [\tau] = \varepsilon[p], \quad [z] = (\eta[\dot{b}]L^2\rho^{-1}g^{-1})^{1/4}, \tag{17a}$$

where ρ is density, g is gravity, and η is ice viscosity, which we consider as constant. We also define the non-dimensional parameters

$$Pe = \lambda^{-1}[z]^2[t]^{-1}, \quad \alpha = [\tau][u](\kappa[T]/[z])^{-1}, \quad \gamma = C[u][\tau]^{-1}, \quad \nu = q_{geo}(\kappa[T]/[z])^{-1}, \tag{17b}$$

$$\varepsilon = [z][x]^{-1}, \quad \delta = [T]T_0^{-1},$$

where Pe is the Péclet number, α is the strength of strain heating compared to the background conductive heat flux, γ is the non-dimensional friction coefficient, ν is the non-dimensional geothermal heat flux, ε is the aspect ratio of the ice sheet, C is the dimensional friction coefficient, q_{geo} is the dimensional geothermal heat flux, and T_0 is the range of temperatures below freezing where subtemperate sliding occurs. For simplicity, we have assumed that ice and bed have the same material properties, so λ is the thermal diffusivity, and κ is the thermal conductivity of the ice.

Dropping stars for simplicity, non-dimensional mass and momentum conservation read

$$\frac{\partial u}{\partial x} + \frac{\partial w}{\partial z} = 0, \tag{18a}$$

$$\varepsilon^2\frac{\partial \tau_{xx}}{\partial x} + \frac{\partial \tau_{xz}}{\partial z} - \frac{\partial p}{\partial x} = -\tan(\mu), \tag{18b}$$

$$\varepsilon^2\left(\frac{\partial \tau_{zx}}{\partial x} + \frac{\partial \tau_{zz}}{\partial z}\right) - \frac{\partial p}{\partial z} = 1, \tag{18c}$$

on $b < z < s$, with the constitutive relationships given by

$$\tau_{xx} = 2\frac{\partial u}{\partial x}, \quad \tau_{zz} = 2\frac{\partial w}{\partial z}, \quad \tau_{xz} = \tau_{zx} = \frac{\partial u}{\partial z} + \varepsilon^2\frac{\partial w}{\partial x}. \tag{18d}$$

The boundary conditions at the ice surface, $z = s$, are

$$-(\varepsilon^2\tau_{xx} - p)\frac{\partial s}{\partial x} + \tau_{xz} = 0, \tag{18e}$$

$$\varepsilon^2\left(-\tau_{xz}\frac{\partial s}{\partial x} + \tau_{zz}\right) - p = 0, \tag{18f}$$

$$\frac{\partial h}{\partial t} + u\frac{\partial s}{\partial x} - w = \dot{b}, \tag{18g}$$

while at the bottom of the ice, $z = b$, we have

$$w = 0, \tag{18h}$$

$$u_b = \gamma^{-1}F(\delta^{-1}T|_{z=0})\tau_b, \tag{18i}$$

with

$$u_b = u, \quad \tau_b = \tau_{xz}. \tag{18j}$$

In the sliding law eq. (18i), $\delta \ll 1$ determines the range of non-dimensional temperature values below the melting point over which sliding is significant, while F is a positive function defined for $T \leq 0$, such that $F' > 0$, and $F \sim O(1)$ when T/δ $O(1)$, with $F(0) = 1$. We note that $F(0) = 1$ implies that the fully-temperate sliding law $u_b = \gamma^{-1}\tau_b$ is recovered when basal temperature reaches the melting point, while the sliding velocity is less than the fully temperate sliding velocity below the melting point.

Energy conservation in the ice and in the bed reads, respectively

$$Pe\left(\frac{\partial T}{\partial t} + u\frac{\partial T}{\partial x} + w\frac{\partial T}{\partial z}\right) - \left(\varepsilon^2\frac{\partial^2 T}{\partial x^2} + \frac{\partial^2 T}{\partial z^2}\right) = \alpha a \qquad b < z < s, \tag{19a}$$

$$Pe\,\frac{\partial T}{\partial t} - \left(\varepsilon^2\frac{\partial^2 T}{\partial x^2} + \frac{\partial^2 T}{\partial z^2}\right) = 0 \qquad -\infty < z < b, \tag{19b}$$

where the strain heating term a is defined as

$$a = 4\varepsilon^2\left(\frac{\partial u}{\partial x}\right)^2 + 4\varepsilon^2\left(\frac{\partial w}{\partial z}\right)^2 + \left(\frac{\partial u}{\partial z}\right)^2 + 2\varepsilon^2\frac{\partial u}{\partial z}w_x + \varepsilon^4\left(\frac{\partial w}{\partial x}\right)^2. \tag{19c}$$

Boundary conditions for the energy balance are

$$T = -1 \qquad \text{on} \quad z = s, \tag{19d}$$

$$[T]_-^+ = 0 \qquad \text{on} \quad z = b, \tag{19e}$$

$$\left[\frac{\partial T}{\partial z}\right]_-^+ + \alpha\, u_b\, \tau_b = 0 \qquad \text{on} \quad z = b \tag{19f}$$

$$\frac{\partial T}{\partial z} \to -\nu \qquad \text{as } z \to -\infty. \tag{19g}$$

The model has six non dimensional parameters: Pe, α, γ, ν, ε, and δ. Similarly to the companion paper, we consider $\alpha, Pe, \gamma, \nu \sim O(1)$, while δ and ε are small. In the following, we use the smallness of δ and ε to derive asymptotically reduced models for the subtemperate region.

We will proceed as follows: first we want to isolate the role of a shallow ice approximation in the instability of the subtemperate region discussed in §1.2. Since there we adopted the limit of $\delta = 0$, for consistency we start by relaxing only the assumption of shallowness, and derive an ice thickness scale model while keeping with the limit of $\delta = 0$ (§2.2). The stability of the resulting thermo-mechanical model is analyzed in §3.

We anticipate here that a Stokes model with subtemperate sliding and $\delta = 0$ remains pathological, and small but finite δ must be considered too. To this aim, in §2.3 we will consider the distinguished limit $\delta \sim \varepsilon^{1/2}$. We will see that in this limit dynamics occur over three distinct length scale: the ice thickness scale, the ice sheet scale, and the geometric average of the two. In §2.3, we derive leading order approximations for ice flow with subtemperate sliding that hold at each of these scales, while we analyze their stability in §§4-5.

2.2 An ice thickness scale model with $\delta = 0$

Let us consider an ice thickness scale ice slab with subtemperate sliding. For this flow, we want to derive a leading order approximation that resolves the ice thickness scale in the horizontal. To this

aim, we introduce the following rescalings in the model (18-19)

$$X = \varepsilon^{-1}x, \quad Z = z - b, \quad \tau = \varepsilon^{-1}t \quad (U, W) = (u, \varepsilon w), \quad H = h = s - b, \quad P = p, \quad \Theta = T, \tag{20a}$$

In addition, we expand dependent variables as

$$\mathbf{U} = \mathbf{U}^{(0)} + O(\varepsilon), \quad H = H^{(0)} + O(\varepsilon), \quad P = H^{(0)} - Z + \varepsilon P^{(1)} + O(\varepsilon^2), \tag{20b}$$

$$\Theta = \Theta^{(0)} + O(\varepsilon), \quad \Theta_b = {\Theta_b}^{(0)} + \delta {\Theta_b}^{(1)} + O(\delta^2)$$

where $H^{(0)}$ is a constant, and Θ_b denotes basal temperature, where we assume ${\Theta_b}^{(0)} = 0$ as a result of $\delta \ll 1$. Then to leading order, and with an error of order $O(\varepsilon)$, we find the Stokes problem

$$\frac{\partial U^{(0)}}{\partial X} + \frac{\partial W^{(0)}}{\partial Z} = 0, \tag{21a}$$

$$\frac{\partial^2 U^{(0)}}{\partial X^2} + \frac{\partial^2 U^{(0)}}{\partial Z^2} - \frac{\partial P^{(1)}}{\partial X} + \tan(\mu) = 0, \tag{21b}$$

$$\frac{\partial^2 W^{(0)}}{\partial X^2} + \frac{\partial^2 W^{(0)}}{\partial W^2} - \frac{\partial P^{(1)}}{\partial Z} = 0, \tag{21c}$$

on $0 < Z < H^{(0)}$, with boundary conditions

$$\frac{\partial U^{(0)}}{\partial Z} + \frac{\partial W^{(0)}}{\partial X} = 0 \qquad \text{on } Z = H^{(0)}, \tag{21d}$$

$$W^{(0)} = 0 \qquad \text{on } Z = H^{(0)}, \tag{21e}$$

$$W^{(0)} = 0 \qquad \text{on } Z = 0. \tag{21f}$$

Note that we have Taylor expanded the stress boundary conditions (18e) about $Z = H^{(0)}$ to obtain the leading order expression (21e).

At this short horizontal length scale, the leading order thermal model, again with an error of order $O(\varepsilon)$, is the advection problem

$$\frac{\partial \Theta^{(0)}}{\partial \tau} + U^{(0)}\frac{\partial \Theta^{(0)}}{\partial X} + W^{(0)}\frac{\partial \Theta^{(0)}}{\partial Z} = 0 \quad \text{on} \quad 0 < Z < H^{(0)}, \tag{21g}$$

where the leading order temperature profile must satisfy, with an error of order $O(\delta)$,

$$\Theta^{(0)} = {\Theta_b}^{(0)} \qquad \text{on} \quad Z = 0, \tag{21h}$$

as well as the Dirichlet condition at the surface

$$\Theta^{(0)} = -1 \quad \text{on} \quad Z = H^{(0)} \tag{21i}$$

The heat equation in the bed simply demands that temperature is independent of τ up to $O(\varepsilon)$, with prescribed heat flux equal to the geothermal one; this, along with continuity of temperature at the bed, yields a leading order temperature profile

$$\Theta^{(0)} = \nu Z, \quad \text{on} \quad Z < 0. \tag{21j}$$

Given that ${\Theta_b}^{(0)} = 0$, the advection problem in the ice can be reduced to an evolution equation for the basal heat flux $\mathcal{Q}$ of the form (see derivation in §3(b) of the companion paper)

$$\frac{\partial \mathcal{Q}^{(0)}}{\partial \tau} + {U_b}^{(0)}\frac{\partial \mathcal{Q}^{(0)}}{\partial X} - \mathcal{Q}^{(0)}\frac{\partial {U_b}^{(0)}}{\partial X} = 0, \tag{21k}$$

where the sliding velocity is implicitely defined by the basal energy budget

$$-\mathcal{Q}^{(0)} + \nu + \alpha {T_b}^{(0)} {U_b}^{(0)} = 0, \tag{21l}$$

where

$${U_b}^{(0)} = U^{(0)}|_{Z=0}, \quad {T_b}^{(0)} = \left(\frac{\partial U^{(0)}}{\partial Z} + \frac{\partial W^{(0)}}{\partial X} \right) \Big|_{Z=0}. \tag{21m}$$

Lastly, the leading order sliding law

$${U_b}^{(0)} = \gamma^{-1} F({\Theta_b}^{(1)}) {T_b}^{(0)} \tag{21n}$$

constrains the first order correction of bed temperature ${\Theta_b}^{(1)}$; we note however that ${\Theta_b}^{(1)}$ does not feed back into the leading order model, hence the sliding law is purely diagnostic when $\delta = 0$.

2.2.1 A faster time scale

An alternative version of the model above, which will be relevant to stability considerations in §3, can be obtained in a similar manner as the model (21), but rescaling time to a faster timescale

$$\mathcal{T} = \varepsilon^{-2} t. \tag{22a}$$

The mechanical model (21a-21f) remains unchanged, except for the kinematic boundary condition at the surface (21e) that is replaced by

$$\frac{\partial H^{(1)}}{\partial \mathcal{T}} - W^{(0)} = 0 \quad \text{on} \quad Z = H^{(0)}, \tag{22b}$$

which forces the leading order velocity field to have dynamics on the fast timescale. The first order ($\sim O(\varepsilon)$) correction of ice thickness $H^{(1)}$ is related to the pressure field through the normal component of the dynamic condition at the surface, which at $O(\varepsilon)$ reads

$$-P^{(1)} + H^{(1)} + \frac{\partial W^{(0)}}{\partial Z} = 0 \quad \text{on} \quad Z = 1. \tag{22c}$$

Coupling to the thermal problem now occurs at first order, where we have, up to an error of order $O(\varepsilon^2)$,

$$\frac{\partial \mathcal{Q}^{(1)}}{\partial \mathcal{T}} + {U_b}^{(0)} \frac{\partial \mathcal{Q}^{(0)}}{\partial X} - \mathcal{Q}^{(0)} \frac{\partial {U_b}^{(0)}}{\partial X} = 0, \tag{22d}$$

while the leading order basal energy budget and the sliding law, eqs. (21l, 21n) remain unchanged, and $\mathcal{Q}^{(0)}$ is independent of the fast time scale $\mathcal{T}$.

2.3 The distinguished limit $\delta \sim \varepsilon^{1/2}$

Here we want to derive a model for the subtemperate ice slab that takes into account $O(\delta)$ deviations of bed temperature from the melting point. The natural distinguished limit to consider is $\delta \sim \varepsilon^{1/2}$, which we adopt throughout the following analysis.

We anticipate here that accounting for such small deviations of bed temperature from the melting point lead to dynamics over a fast timescale $\tau = t/\varepsilon$; this is the timescale we will consider throughout §2.3. Furthermore, these dynamics occur over three distinct horizontal length scales, namely the ice thickness scale, the ice sheet scale, and a length scale intermediate between the two. In the following we derive leading order approximations to the thermo-mechanical model (18-19) rescaled to the fast timescale τ at each of these length scales.

2.3.1 Ice thickness scale

The derivation of a leading order model valid at the ice thickness scale follows the derivation in §2.2. The leading order mechanical problem is given by eqs. (21a-21f) along with the sliding law (21n), while the leading order thermal problem is given by the advection-only model (21k), with the basal energy budget (21l).

The advection-only outer problem (21k) ignores $O(\delta)$ deviations of basal temperature from the melting point, ${\Theta_b}^{(1)}$, which are indeed required in the sliding law (21n). In order to formulate a model for the evolution of ${\Theta_b}^{(1)}$, we need to resort to a thermal boundary layer near the bed. Assuming the distinguished limit $\delta \sim \varepsilon^{1/2}$, and rescaling the master model (19) as

$$\tilde{X} = \varepsilon^{-1} x, \quad \tilde{Z} = \delta^{-1} z, \quad \tau = \varepsilon^{-1} t, \quad \tilde{\Theta} = \delta^{-1} T, \quad (\tilde{U}, \tilde{W}) = (u, \varepsilon \delta^{-1} w), \tag{23a}$$

and also expanding near the bed as

$$(\tilde{U}, \tilde{W}) = \left({U_b}^{(0)} + O(\delta), -\frac{\partial {U_b}^{(0)}}{\partial X} \tilde{Z} + O(\delta^2) \right), \quad \tilde{\Theta} = \tilde{\Theta}^{(0)} + O(\delta), \tag{23b}$$

we find the following leading order problem for $\tilde{\Theta}$, correct up to an error of $O(\varepsilon)$

$$\frac{\partial \tilde{\Theta}^{(0)}}{\partial \tau} + {U_b}^{(0)} \frac{\partial \tilde{\Theta}^{(0)}}{\partial \tilde{X}} - \frac{\partial {U_b}^{(0)}}{\partial X} \tilde{Z} \frac{\partial \tilde{\Theta}^{(0)}}{\partial \tilde{Z}} - \frac{\partial^2 \tilde{\Theta}^{(0)}}{\partial \tilde{Z}^2} = 0 \quad \text{for } \tilde{Z} > 0, \tag{24a}$$

$$\frac{\partial \tilde{\Theta}^{(0)}}{\partial \tau} - \frac{\partial^2 \tilde{\Theta}^{(0)}}{\partial \tilde{Z}^2} = 0 \quad \text{for } \tilde{Z} < 0, \tag{24b}$$

with boundary conditions at the bed

$$\left[\tilde{\Theta}^{(0)} \right]_-^+ = 0 \qquad \text{on} \quad \tilde{Z} = 0, \tag{24c}$$

$$\left[\frac{\partial \tilde{\Theta}^{(0)}}{\partial \tilde{Z}} \right]_-^+ + \alpha \, {U_b}^{(0)} \, {T_b}^{(0)} = 0, \qquad \text{on} \quad \tilde{Z} = 0, \tag{24d}$$

and matching conditions

$$-\frac{\partial \tilde{\Theta}^{(0)}}{\partial \tilde{Z}} \to \mathcal{Q}^{(0)} \quad \text{as} \quad \tilde{Z} \to +\infty, \quad -\frac{\partial \tilde{\Theta}^{(0)}}{\partial \tilde{Z}} \to \nu \quad \text{as} \quad \tilde{Z} \to -\infty. \tag{24e}$$

Recalling that, through the rescalings (23a), ${\Theta_b}^{(1)} = \tilde{\Theta}^{(0)}(\tilde{Z} = 0)$, it's straightforward to recognize that the model above effectively constrains the first order deviation of bed temperature from the melting point, which is required in the computation of the sliding velocity through the sliding law (21n).

2.3.2 An intermediate horizontal scale

We now consider a horizontal length scale intermediate between the ice thickness scale and the ice sheet scale,

$$\mathsf{X} = \varepsilon^{-1/2} x. \tag{25a}$$

We rescale the master model (18-19) as

$$\mathsf{z} = z - b, \quad \tau = \varepsilon^{-1} t \quad (\mathsf{u}, \mathsf{w}) = (u, \varepsilon^{1/2} w), \quad \mathsf{h} = h = s - b, \quad \mathsf{p} = p, \quad \mathsf{T} = T, \quad \mathsf{T}_b = T|_{z=0}, \tag{25b}$$

and also expand dependent variables as

$$\mathbf{u} = (\mathsf{u}, \mathsf{w}) = \mathbf{u}^{(0)} + O(\varepsilon^{1/2}), \quad \mathsf{h} = \mathsf{h}^{(0)} + \varepsilon^{1/2}\mathsf{h}^{(1)} + O(\varepsilon), \quad \mathsf{p} = \mathsf{h}^{(0)} - \mathsf{z} + \varepsilon^{1/2}\mathsf{h}^{(1)} + O(\varepsilon), \tag{25c}$$

$$\mathsf{T} = \mathsf{T}^{(0)} + O(\varepsilon^{1/2}), \quad \mathsf{T}_b = {\mathsf{T}_b}^{(0)} + \delta {\mathsf{T}_b}^{(1)} + O(\delta^2)$$

where $\mathsf{h}^{(0)}$. Over this fast time scale, the leading order mechanical model is a shallow ice model, which however differs from the standard, ice sheet scale version in that it links the first order correction of the ice thickness, $\mathsf{h}^{(1)}$, to the leading order horizontal velocity, $\mathsf{u}^{(0)}$. With an error of order $O(\varepsilon^{1/2})$, the horizontal velocity is the solution to

$$\frac{\partial^2 \mathsf{u}^{(0)}}{\partial \mathsf{z}^2} = -\tan(\mu) + \frac{\partial \mathsf{h}^{(1)}}{\partial \mathsf{x}} \qquad \text{on} \quad 0 < \mathsf{z} < \mathsf{h}^{(0)}, \tag{25d}$$

$$\mathsf{u}^{(0)} = {\mathsf{u}_b}^{(0)} \qquad \text{on} \quad \mathsf{z} = 0, \tag{25e}$$

$$\frac{\partial \mathsf{u}^{(0)}}{\partial \mathsf{z}} = 0 \qquad \text{on} \quad \mathsf{z} = \mathsf{h}^{(0)}, \tag{25f}$$

which can be integrated straightforwardly to yield

$$\mathsf{u}^{(0)} = -\frac{1}{2}\left({\mathsf{h}^{(0)}}^2 - \left(\mathsf{h}^{(0)} - \mathsf{z}\right)^2\right)\left(\frac{\partial \mathsf{h}^{(1)}}{\partial \mathsf{x}} - \tan(\mu)\right) + {\mathsf{u}_b}^{(0)}, \tag{25g}$$

where

$${\mathsf{u}_b}^{(0)} = \gamma^{-1} F({\mathsf{T}_b}^{(1)}) {\mathsf{t}_b}^{(0)}, \quad \text{with} \quad {\mathsf{t}_b}^{(0)} = -\mathsf{h}^{(0)}\left(\frac{\partial \mathsf{h}^{(1)}}{\partial \mathsf{x}} - \tan(\mu)\right). \tag{25h}$$

Equipped with the latter expression for the horizontal velocity, we can link the vertical velocity to the horizontal velocity by depth-integration of the leading order mass conservation with bed impermeability

$$\frac{\partial \mathsf{u}^{(0)}}{\partial \mathsf{x}} + \frac{\partial \mathsf{w}^{(0)}}{\partial \mathsf{z}} = 0 \quad \text{on} \quad 0 < \mathsf{z} < \mathsf{h}^{(0)}, \quad \mathsf{w}^{(0)} = 0 \quad \text{on } \mathsf{z} = 0, \tag{25i}$$

which yields an expression for the vertical velocity at the surface as a function of the mass flux

$$\mathsf{w}^{(0)}|_{\mathsf{z}=\mathsf{h}^{(0)}} = -\frac{\partial \mathsf{q}^{(0)}}{\partial \mathsf{x}}, \quad \mathsf{q}^{(0)} = \int_{\mathsf{z}=0}^{\mathsf{z}=\mathsf{h}^{(0)}} \mathsf{u}^{(0)}\, \mathrm{d}\mathsf{z} + {\mathsf{u}_b}^{(0)}\mathsf{h}^{(0)}. \tag{25j}$$

Lastly, the kinematic boundary condition along with (25j) provides the desired link between ice thickness and the mass flux through the diffusion equation

$$\frac{\partial \mathsf{h}^{(1)}}{\partial \tau} + \frac{\partial \mathsf{q}^{(0)}}{\partial \mathsf{x}} = 0. \tag{25k}$$

The leading order thermal model, with an error of order $O(\varepsilon^{1/2})$, reduces to

$$\frac{\partial \mathsf{T}^{(0)}}{\partial \tau} = 0 \quad \text{on} \quad -\infty < \mathsf{z} < \mathsf{h}^{(0)}, \tag{25l}$$

where $\mathsf{T}^{(0)}$ must satisfy

$$\mathsf{T}^{(0)} = -1 \qquad \text{on} \quad \mathsf{z} = \mathsf{h}^{(0)}, \tag{25m}$$

$$\mathsf{T}^{(0)} = {\mathsf{T}_b}^{(0)} \qquad \text{on} \quad \mathsf{z} = 0, \tag{25n}$$

$$-\frac{\partial \mathsf{T}^{(0)}}{\partial \mathsf{z}} \to \nu \qquad \text{as} \quad \mathsf{z} \to -\infty, \tag{25o}$$

where ${\mathsf{T}_b}^{(0)} = 0$. In order to close the model we need an evolution equation for the first order correction to basal temperature, ${\mathsf{T}_b}^{(1)}$, which is once again constrained by a basal thermal boundary layer. To derive a leading order approximation valid at this intermediate length scale, we rescale the full model (18-19) as

$$\tilde{\mathsf{x}} = \varepsilon^{-1/2}x, \quad \tilde{\mathsf{z}} = \delta^{-1}z, \quad \tilde{\mathsf{T}} = \delta^{-1}T, \quad (\tilde{\mathsf{u}}, \tilde{\mathsf{w}}) = (u, \delta^{-1}\varepsilon^{1/2}w), \tag{25p}$$

where we put $\delta \sim \varepsilon^{1/2}$, and also expand as

$$(\tilde{\mathsf{u}}, \tilde{\mathsf{w}}) = \left({\mathsf{u}_b}^{(0)} + O(\tilde{\mathsf{z}}), O(1)\right), \quad \tilde{\mathsf{T}} = \tilde{\mathsf{T}}^{(0)} + O(\delta) \tag{25q}$$

whereby ${\mathsf{T}_b}^{(1)} = \tilde{\mathsf{T}}^{(0)}(\tilde{\mathsf{z}} = 0)$. The leading order problem correct up to an error of order $O(\varepsilon^{1/2})$ is

$$\frac{\partial \tilde{\mathsf{T}}^{(0)}}{\partial \tau} - \frac{\partial^2 \tilde{\mathsf{T}}^{(0)}}{\partial \tilde{\mathsf{z}}^2} = 0 \quad \text{for} \quad -\infty < \tilde{\mathsf{z}} < 0 \quad \text{and} \quad 0 < \tilde{\mathsf{z}} < +\infty, \tag{25r}$$

with boundary conditions at the bed

$$\left[\tilde{\mathsf{T}}^{(0)}\right]_-^+ = 0 \qquad \text{on} \quad \tilde{\mathsf{z}} = 0, \tag{25s}$$

$$\left[\frac{\partial \tilde{\mathsf{T}}^{(0)}}{\partial \tilde{\mathsf{z}}}\right]_-^+ + \alpha\, \mathsf{u}^{(0)}{\mathsf{t}_b}^{(0)} = 0, \qquad \text{on } \tilde{\mathsf{z}} = 0, \tag{25t}$$

and matching conditions

$$\frac{\partial \tilde{\mathsf{T}}^{(0)}}{\partial \tilde{\mathsf{z}}} \to 0 \quad \text{as} \quad \tilde{\mathsf{z}} \to +\infty, \quad -\frac{\partial \tilde{\mathsf{T}}^{(0)}}{\partial \tilde{\mathsf{z}}} \to \nu \quad \text{as} \quad \tilde{\mathsf{z}} \to -\infty. \tag{25u}$$

2.3.3 Ice sheet scale

The derivation of a leading order approximation to the full model (18-19) with the fast timescale $\tau = t/\varepsilon$ at the ice sheet scale is straightforward, and follows the derivation of the intermediate scale model (25). Below we provide only the leading order approximation at the ice sheet scale.

Keeping with the same notation as in eqs.(17) for simplicity, the leading order horizontal velocity is given by

$$u^{(0)} = -\frac{1}{2}\left[{h^{(0)}}^2 - \left(h^{(0)} - z\right)^2\right]\left(\frac{\partial h^{(0)}}{\partial x} - \tan(\mu)\right) + {u_b}^{(0)}, \tag{26a}$$

with

$${u_b}^{(0)} = \gamma^{-1}F({T_b}^{(1)}){\tau_b}^{(0)}, \quad \text{with} \quad {\tau_b}^{(0)} = -h^{(0)}\left(\frac{\partial h^{(0)}}{\partial x} - \tan(\mu)\right), \tag{26b}$$

and leading order ice thickness independent of the fast time variable, namely

$$\frac{\partial h^{(0)}}{\partial \tau} = 0. \tag{26c}$$

As for the thermal problem, the outer flux $Q^{(0)} = -\partial T^{(0)}/\partial z|_{z=0}$ is also independent of the fast time variable

$$\frac{\partial Q^{(0)}}{\partial \tau} = 0, \tag{26d}$$

so that, once again, the thermal problem is governed by a thin ($\sim \delta$) boundary layer near the bed. We denote variables in the thermal boundary layer with $\tilde{\cdot}$, and rescale as

$$\tilde{x} = x, \quad \tilde{z} = \delta^{-1} z, \quad \tilde{T} = \delta^{-1} T, \quad (\tilde{u}, \tilde{w}) = (u, \delta^{-1} w), \tag{26e}$$

whereby ${T_b}^{(1)} = \tilde{T}(\tilde{z} = 0)$. In addition, near the bed we can expand dependent variables as

$$(\tilde{u}, \tilde{w}) = \left({u_b}^{(0)} + O(\delta), O(1)\right), \quad \tilde{T} = \tilde{T}^{(0)} + O(\delta), \tag{26f}$$

which yields the leading order boundary layer problem correct up to order $O(\varepsilon)$

$$\frac{\partial \tilde{T}^{(0)}}{\partial \tau} - \frac{\partial^2 \tilde{T}^{(0)}}{\partial \tilde{z}^2} = 0 \quad \text{for} \quad -\infty < \tilde{z} < 0 \quad \text{and} \quad 0 < \tilde{z} < +\infty, \tag{26g}$$

with boundary conditions at the bed

$$\left[\tilde{T}^{(0)}\right]_-^+ = 0 \qquad \text{on} \quad \tilde{z} = 0, \tag{26h}$$

$$\left[\frac{\partial \tilde{T}^{(0)}}{\partial \tilde{z}}\right]_-^+ + \alpha\, {u_b}^{(0)} {\tau_b}^{(0)} = 0, \qquad \text{on } \tilde{z} = 0, \tag{26i}$$

and matching conditions

$$\frac{\partial \tilde{T}^{(0)}}{\partial \tilde{z}} \to 0 \quad \text{as} \quad \tilde{z} \to +\infty, \quad -\frac{\partial \tilde{T}^{(0)}}{\partial \tilde{z}} \to \nu \quad \text{as} \quad \tilde{z} \to -\infty. \tag{26j}$$

3 Stability of the ice thickness scale problem with $\delta = 0$

3.1 Model reformulation

In this section we are concerned with a linear stability analysis of the ice thickness scale model with $\delta = 0$ described by eqs. (21 - 22). To facilitate the solution of the mechanical model, we reformulate the Stokes problem (21a-21f) in terms of a streamfunction ψ defined as

$$U^{(0)} = \frac{\partial \psi}{\partial Z}, \quad W^{(0)} = -\frac{\partial \psi}{\partial X}, \tag{27a}$$

so that sliding velocity and basal shear stress read

$${U_b}^{(0)} = \left.\frac{\partial \psi}{\partial Z}\right|_{Z=0}, \quad {T_b}^{(0)} = \left.\frac{\partial^2 \psi}{\partial Z^2}\right|_{Z=0}. \tag{27b}$$

In addition, and with the objective to reduce the number of parameters, we introduce the rescalings

$$(Z^*, X^*, {H^{(1)}}^*) = (Z, X, H^{(1)})/H^{(0)}, \quad (\tau^*, \mathcal{T}^*) = (\tau, \mathcal{T}) q^{(0)}/(H^{(0)})^2, \quad {P^*}^{(1)} = P^{(1)} (H^{(0)})^2/q^{(0)},$$
$$\psi^* = \psi/q^{(0)}, \quad ({\mathcal{Q}^*}^{(0)}, {\mathcal{Q}^*}^{(1)}) = (\mathcal{Q}^{(0)}, \mathcal{Q}^{(1)}) \quad \gamma^* = \gamma H^{(0)}, \quad \nu^* = \nu H^{(0)}, \quad \alpha^* = \alpha (q^{(0)}/H^{(0)})^2 \tag{27c}$$

where $H^{(0)}$ and $q^{(0)}$ are the leading order ice thickness and mass flux, which we recall to be independent of X and τ. Under the latter rescalings, the subtemperate slab will have unitary ice thockness and ice flux.

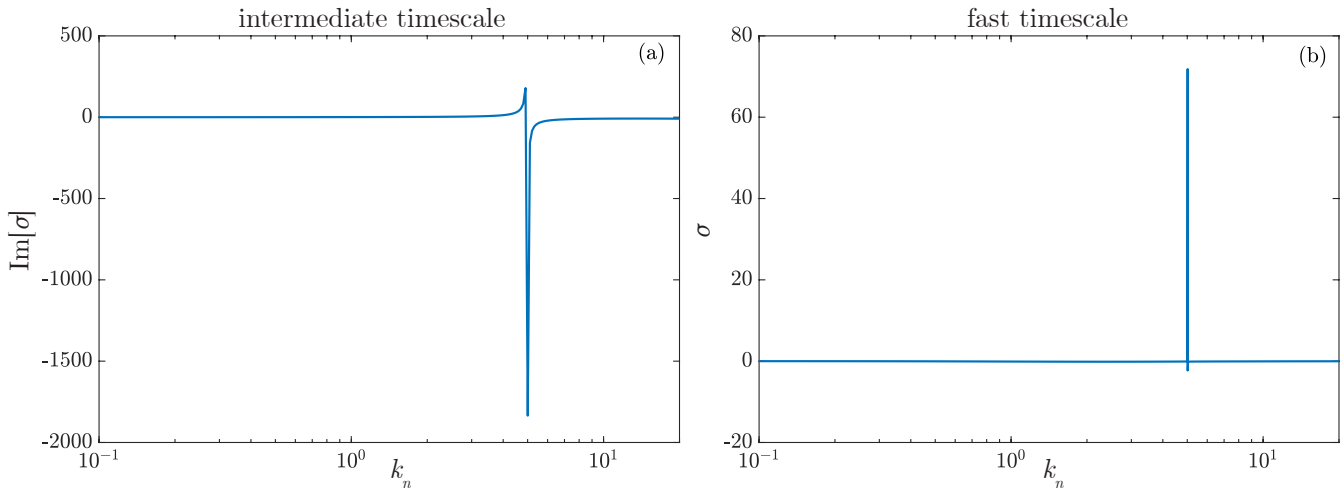

Figure 1: Eigenvalue for the ice thickness scale model with $\delta = 0$. Panel (a): intermediate time scale, $t \sim \varepsilon^{-1}$. Panel (b): fast time scale, $t \sim \varepsilon^{-2}$. Parameters are $\nu = 1$, $\alpha = 1$, $\gamma = 10$ ($\bar{U}_b = 0.231$, so we are in the slow sliding regime).

Rescaling variables as described by eqs. (27c) and dropping asterisks immediately thereafter, the mechanical model can be reduced to the biharmonic problem [7]

$$\nabla^4 \psi = 0 \quad \text{on} \quad 0 < Z < 1, \tag{27d}$$

with boundary conditions

$$\frac{\partial^2 \psi}{\partial Z^2} - \frac{\partial^2 \psi}{\partial X^2} = 0 \qquad \text{on} \quad Z = 1, \tag{27e}$$

$$\frac{\partial^2 \psi}{\partial X^2} = 0 \qquad \text{on} \quad Z = 1, \tag{27f}$$

$$\frac{\partial^2 \psi}{\partial X^2} = 0 \qquad \text{on} \quad Z = 0, \tag{27g}$$

$$\frac{\partial \psi}{\partial Z} = \frac{F(\Theta_b{}^{(1)})}{\gamma} \frac{\partial^2 \psi}{\partial Z^2} \qquad \text{on} \quad Z = 0. \tag{27h}$$

For the fast timescale version of the mechanical model, eqs. (22), the condition (27f) is replaced by

$$\frac{\partial H^{(1)}}{\partial \mathcal{T}} + \frac{\partial^2 \psi}{\partial X^2} = 0 \quad \text{on} \quad Z = 1, \tag{27i}$$

with $H^{(1)}$ constrained by

$$-P^{(1)} + \frac{(H^{(0)})^3}{q^{(0)}} H^{(1)} - \frac{\partial^2 \psi}{\partial X \partial Z} = 0 \quad \text{on} \quad Z = 1. \tag{27j}$$

After rescaling and dropping asterisks, the advection-only model (21k) with the basal energy budget (21l) remain unchanged.

3.2 An intermediate time scale, $t \sim \varepsilon^{-1}$

Here we perform a stability analysis of the model (21) reformulated as described above. For simplicity, we assume a periodic domain of length L and expand dependent variables as

$$\psi = \bar{\psi} + \beta \psi', \quad T_b = \bar{T}_b + \beta T_b', \quad P^{(1)} = \beta P', \quad \mathcal{Q}^{(0)} = \bar{\mathcal{Q}} + \beta \mathcal{Q}', \beta \ll 1, \tag{28a}$$

where barred quantities do not depend on X and τ; we Fourier-transform perturbations in X as

$$\hat{g}_n(Z,\tau) = \frac{1}{L}\int_0^L g'(X,Z,\tau)\exp\left(-ik_nX\right)\mathrm{d}X, \quad k_n = \frac{2\pi n}{L}. \tag{28b}$$

where, by separation of variables, we also take $\partial\hat{f}_n/\partial\tau = \sigma\hat{f}_n$. This yields the following $O(\beta)$ problem for $\hat{\psi}_n$

$$k_n^4\hat{\psi}_n + \frac{\partial^4\hat{\psi}_n}{\partial Z^4} - 2k_n^2\frac{\partial^2\hat{\psi}_n}{\partial Z^2} = 0 \qquad \text{on } 0 < Z < 1, \tag{28c}$$

$$\frac{\partial^2\hat{\psi}_n}{\partial Z^2} + k_n^2\hat{\psi}_n = 0 \qquad \text{on } Z = 1, \tag{28d}$$

$$\hat{\psi}_n = 0 \qquad \text{on } Z = 1, \tag{28e}$$

$$\hat{\psi}_n = 0 \qquad \text{on } Z = 0, \tag{28f}$$

where we omitted the sliding law as it does not feed back in the leading order problem for $\delta = 0$. The heat transport problem reads

$$\sigma\hat{Q}_n + ik_n\bar{U}_b\hat{Q}_n - ik_n\bar{Q}\hat{U}_{b,n} = 0, \tag{28g}$$

with basal energy budget

$$-\hat{Q}_n + \alpha\left(\bar{U}_b\hat{T}_{b,n} + \bar{T}_b\hat{U}_{b,n}\right) = 0, \tag{28h}$$

and

$$\hat{U}_{b,n} = \left.\frac{\partial\hat{\psi}_n}{\partial Z}\right|_{Z=0}, \quad \hat{T}_{b,n} = \left.\frac{\partial^2\hat{\psi}_n}{\partial Z^2}\right|_{Z=0}. \tag{28i}$$

3.2.1 Solution

The Fourier-transformed biharmonic equation has general solution

$$\hat{\psi}_n = (A + BZ)\exp\left(-k_nZ\right) + (C + DZ)\exp\left(k_nZ\right), \tag{28j}$$

with integration constants

$$B = -\frac{A}{2}\left(1 - \exp\left(2k_n\right)\right), \quad C = -A, \quad D = \frac{A}{2}\left(1 - \exp\left(-2k_n\right)\right), \tag{28k}$$

where we set $A = 1$ in the light of the biharmonic problem being homogeneous. Then, substituting the latter expression in the linearized version of (27b), we obtain the following expressions for the perturbed sliding velocity and basal shear stress,

$$\hat{U}_{b,n} = -2k_n + \sinh\left(2k_n\right), \quad \hat{T}_{b,n} = -4k_n\sinh\left(k_n\right)^2. \tag{28l}$$

which we use to compute $\hat{Q}_n$ from eq. (28h). Finally, the $Q-$equation (28g) yields the purely imaginary eigenvalue

$$\sigma = i\frac{\left(\bar{Q} - \alpha\bar{U}_b\bar{T}_b\right)\left[2k_n^2 - k_n\sinh\left(2k_n\right)\right] - 4\alpha\bar{U}_b^2k_n^4\sinh\left(k_n\right)^2}{2\alpha k_n\left[\bar{T}_b + 2\bar{U}_b\sinh\left(k_n\right)^2\right] - \alpha\bar{T}_b\sinh\left(2k_n\right)}. \tag{28m}$$

Even though the stability analysis is inconclusive with respect to the growth or decay of perturbations, it is straightforward to demonstrate that, at least for slow sliding, this model is pathological, as suggested by the plot of $\mathrm{Im}[\sigma]$ shown in panel (a) of figure 1, which displays a singularity for $k_n \approx 5$.

To understand the origin of the singularity, we Taylor-expand the denominator of eq. (28m) about $k_n = 0$, leading to

$$2\alpha k_n \left[\bar{T}_b + 2\bar{U}_b \sinh\left(k_n\right)^2\right] - \alpha \bar{T}_b \sinh\left(2k_n\right) \sim 4\left(-\frac{\bar{T}_b}{3} + \bar{U}_b\right) k_n^3. \tag{28n}$$

Recalling that the Stokes problem has been rescaled so as to obtain a unitary steady state ice thickness, we recognize that the term in brackets is the difference between the mass flux by sliding, $\bar{U}_b$, and the mass flux by internal deformation, $\bar{T}_b/3$, which is negative for slow sliding. Consider now a short wavelength limit, $k_n \to +\infty$. For $k_n \to +\infty$ the denominator of eq. (28m) diverges to positive infinity,

$$2\alpha k_n \left[\bar{T}_b + 2\bar{U}_b \sinh\left(k_n\right)^2\right] - \alpha \bar{T}_b \sinh\left(2k_n\right) \sim 4k_n \bar{U}_b \sinh\left(k_n\right)^2, \tag{28o}$$

thus implying the existence of a zero for some finite k_n in the denominator of eq. (28m), at least for slow sliding. As for the numerator of eq. (28m), recalling that in a steady state $\bar{Q} - \alpha \bar{U}_b = \nu$ is a positive quantity and that $\sinh(k_n)$ is strictly positive for $k_n > 0$, and also noting that the first term vanishes for $k_n \to 0$, we conclude that the numerator behaves as $\sim -k_n^4$ with negative derivative for $k_n \to 0$ and diverges exponentially to negative infinity for $k_n \to +\infty$, so it does not have zeros for $k_n > 0$. As a result, we expect that at least for slow sliding σ becomes infinite for some finite k_n, meaning that perturbations of the system would propagate at infinite wavespeed. This insight is confirmed by the solution shown in panel (a) of figure 1, and generalizes to the entire slow sliding regime.

3.3 A fast time scale, $t \sim \varepsilon^{-2}$

The stability analysis for the intermediate time scale suggests that the ice thickness scale model with $\delta = 0$ might be well behaved in the fast sliding regime. In this section we are going to show that this is not the case, and that an instability exists at the fast timescale $\mathcal{T} = t\varepsilon^{-2}$ that renders the model pathological regardless of whether sliding is slow or fast.

We intend to perform a stability analysis of the ice thickness scale model with $\delta = 0$ and fast time scale described in §2.2.1. Recalling that $Q^{(0)}$ is independent of $\mathcal{T}$ and X, we expand dependent variables about their steady state as

$$\psi = \bar{\psi} + \beta\psi', \quad T_b = \bar{T}_b + \beta T_b', \quad P^{(1)} = \beta P', \quad \mathcal{Q}^{(1)} = \beta \mathcal{Q}', \quad H^{(1)} = \beta H', \quad \beta \ll 1, \tag{29a}$$

where barred quantities are independent of X and $\mathcal{T}$; we also Fourier-transform perturbed variables in X (assuming once again a periodic domain) as

$$\hat{g}_n(Z, \mathcal{T}) = \frac{1}{L}\int_0^L g'(X, Z, \mathcal{T}) \exp\left(-ik_n X\right) \mathrm{d}X, \quad k_n = \frac{2\pi n}{L}. \tag{29b}$$

where, by separation of variables, we take $\partial \hat{g}_n / \partial \mathcal{T} = \sigma \hat{g}_n$.

Then to $O(\beta)$ we obtain eqs. (28c-28d, 28f), whereas eq. (28e) is replaced by the kinematic boundary condition

$$\sigma \hat{H}_n + ik_n \hat{\psi}_n = 0 \quad \text{on } Z = 1, \tag{29c}$$

with the perturbation of the ice thickness constrained by

$$-\hat{P}_n + \frac{\bar{H}^3}{\bar{q}}\hat{H}_n - ik_n\frac{\partial\hat{\psi}_n}{\partial Z} = 0 \quad \text{on} \quad Z = 1, \tag{29d}$$

where $\bar{H} = H^{(0)}$, $\bar{q} = q^{(0)}$. The thermal problem is

$$\sigma\hat{Q}_n - ik_nQ^{(0)}\hat{U}_{b,n} = 0, \tag{29e}$$

with basal energy budget

$$\bar{U}_b\hat{T}_{b,n} + \bar{T}_b\hat{U}_{b,n} = 0, \tag{29f}$$

and

$$\hat{U}_{b,n} = \left.\frac{\partial\hat{\psi}_n}{\partial Z}\right|_{Z=0}, \quad \hat{T}_{b,n} = \left.\frac{\partial^2\hat{\psi}_n}{\partial Z^2}\right|_{Z=0}. \tag{29g}$$

3.3.1 Solution

The general solution of the perturbed biharmonic equation is eq. (28j). Enforcing boundary conditions (28d,28f, 29c) leads to integration constants

$$\begin{aligned} B = -\frac{A}{2}\left[1 - \exp\left(2k_n\right)\right] + \frac{(1+k_n)i\sigma\hat{H}_n\exp\left(k_n\right)}{2k_n}, \quad C = -A, \\ D = \frac{A}{2}\left[1 - \exp\left(-2k_n\right)\right] + \frac{(1-k_n)i\sigma\hat{H}_n\exp\left(-k_n\right)}{2k_n}, \end{aligned} \tag{30a}$$

where we set $A = 1$ in the light of the biharmonic problem being homogeneous. With an expression for the stream function, we compute pressure from momentum conservation in the horizontal direction, which at $O(\beta)$ reads

$$-k_n^2\frac{\partial\hat{\psi}_n}{\partial\hat{Z}} + \frac{\partial\hat{\psi}_n}{\partial Z^3} - ik_n\hat{P}_n = 0. \tag{30b}$$

Differentiating the solution, we get

$$\hat{P}_n = 2\left[ik_n(\sinh\left(k_n(-2+Z)\right) - \sinh\left(k_nZ\right)) + \sigma\hat{H}_n(\cosh\left(k_n - k_nZ\right) + k_n\sinh\left(k_n - k_nZ\right))\right], \tag{30c}$$

which we substitute into eq. (29d) to find the perturbation of the free surface

$$\hat{H}_n = \frac{q^{(0)}}{(H^{(0)})^3}\left[\frac{4ik_n^2\cosh\left(k_n\right)}{-1 + 2k_n^2\sigma}\right]. \tag{30d}$$

Last, the basal energy budget eq. (29f) yields a real eigenvalue of the form

$$\sigma = -\frac{\bar{U}_b\left[1 - \cosh\left(2k_n\right)\right] - \bar{T}_b + \bar{T}_b(2k_n)^{-1}\sinh\left(2k_n\right)}{\bar{T}_b + 2k_n^2\left(-2\bar{U} + \bar{T}_b\right) + \bar{T}_b\cosh\left(2k_n\right) - 2k_n\bar{U}_b\sinh\left(2k_n\right)}, \tag{30e}$$

whereby $\hat{Q}_n$ can be computed straightforwardly from eq. (29e). The behaviour of σ as a function of k_n is illustrated in panel (b) of figure 1.

To understand the properties of the model we first consider short and long wavelength limits of eq. (30e). We start from the limit of small k_n, where we expect that the stability features of the Stokes problem correspond to those of the shallow ice problem. Taylor-expanding eq. (30e) about $k_n = 0$, we find

$$\sigma \sim \bar{T}_b^{-1} \left(-\frac{\bar{T}_b}{3} + \bar{U}_b \right) k_n^2 + O(k_n^4) \quad \text{as } k_n \to 0. \tag{30f}$$

Recalling that the we rescaled the ice thickness scale problem so as to obtain a unitary steady state ice thickness and ice flux, we recognize that the term in brackets in the expression above is the difference between the mass flux by sliding, $\bar{U}_b$, and the mass flux by internal deformation, $\bar{T}_b/3$. Therefore the ice thickness scale model is stable to long wavelength perturbations for slow sliding and unstable otherwise, consistently with the limiting behaviour for short wavelength perturbations that we identified in the shallow-ice subtemperate slab model (see §1.2).

Short wavelength perturbations, corresponding to the limiting case $k_n \to \infty$, are neutrally stable with this scaling,

$$\sigma \sim -\frac{1}{k_n} \quad \text{as } k_n \to +\infty, \tag{30g}$$

thus confirming that extensional stresses provide damping of perturbations, and backward diffusion is no longer an issue. Nonetheless, we are now going to show that the model remains pathological, regardless of the stabilizing effect of extensional stresses: in fact, we will find that the eigenvalue becomes infinite for $O(1)$ wavelength, so no well-behaved solution exists.

This is straightforward to appreciate by looking at the denominator of eq. (30e): for $k_n = 0$ it takes the positive value $2\bar{T}_b$, whereas for large k_n it diverges to negative infinity as $\sim -k_n \sinh(2k_n)$. It thus follows that the denominator of eq. (30e) must have a zero for some finite value of k_n, so we expect σ to become infinite as a result. This is consistent with the plot of σ shown in panel (b) of figure 1, which displays a singularity for $k_n \approx 4$. Note that our argument does not depend on whether sliding is slow or fast, and the singular behaviour persists in both regimes.

4 Stability of the ice thickness scale problem with $\delta \sim \varepsilon^{1/2}$

4.1 Stability analysis

In this section we are concerned with a linear stability analysis of the ice thickness scale model with finite δ described in §2.3.1. To facilitate the solution of the mechanical model, we proceed like in §3.1; replacing the rescalings (27c) with

$$(Z^*, \hat{Z}^*) = (Z, \tilde{Z})/H^{(0)}, \quad (X^*, \hat{X}^*) = (X, \tilde{X})/H^{(0)}, \quad \tau^* = \tau q^{(0)}/(H^{(0)})^2, \tag{31}$$

$$\psi^* = \psi/q^{(0)}, \quad (\hat{\Theta^*}^{(0)}, \mathcal{Q}^{*(0)}) = (\tilde{\Theta}^{(0)}, \mathcal{Q}^{(0)}) \quad \gamma^* = \gamma H^{(0)}, \quad \nu^* = \nu H^{(0)}, \quad \alpha^* = \alpha (q^{(0)}/H^{(0)})^2$$

and dropping both asterisks and superscripts for simplicity, we obtain the mechanical model (27d-27h) while the thermal model (24) remains unchanged under rescalings.

4.1.1 Steady state and linearization

In the usual linear stability framework, we consider small amplitude perturbations about the steady state, so we expand dependent variables as $g = \bar{g} + \beta g'$, where $\bar{g}$ is independent of τ. To $O(1)$ we

find the spatially-uniform steady state

$$\bar{U}_b = \frac{3\bar{F}}{\gamma + 3\bar{F}}, \quad \bar{\tilde{\Theta}} = \begin{cases} \Theta_{bed} - \bar{\mathcal{Q}}\tilde{Z} & \text{for } \tilde{Z} > 0 \\ \Theta_{bed} - \nu\tilde{Z} & \text{for } \tilde{Z} < 0 \end{cases}, \quad \bar{\mathcal{Q}} = \nu + \alpha\bar{T}_b\bar{U}_b, \quad \bar{T}_b = 3(1 - \bar{U}_b), \tag{32a}$$

where $\bar{F} = F(\Theta_{bed})$. Assuming once again a periodic domain of length L, we Fourier-transform the perturbations in X as

$$\hat{g}(Z,\tau) = \frac{1}{L}\int_0^L g'(X,Z,\tau)\exp\left(-ik_nX\right)\mathrm{d}X, \quad k_n = \frac{2\pi n}{L} \tag{32b}$$

The linearized, $O(\beta)$ mechanical problem is given by eqs. (28c- 28f), with sliding law

$$\hat{U}_{b,n} = \gamma^{-1}\left(\bar{F}\hat{T}_{b,n} + \bar{T}_b\tilde{F}'\hat{\tilde{\Theta}}_n|_{\tilde{Z}=0}\right), \tag{32c}$$

where $F' = \mathrm{d}F/\mathrm{d}\Theta|_{\bar{\Theta}}$ is a strictly positive function. Lastly, the linearized thermal problem is

$$\frac{\mathrm{d}\hat{\mathcal{Q}}_n}{\mathrm{d}\tau} + ik_n\left(\bar{U}_b\hat{\mathcal{Q}}_n - \bar{\mathcal{Q}}\hat{U}_{b,n}\right) = 0, \tag{33a}$$

$$\frac{\partial\hat{\tilde{\Theta}}_n}{\partial\tau} + ik_n\left(\bar{U}_b\hat{\tilde{\Theta}}_n + \bar{\mathcal{Q}}\hat{U}_{b,n}\tilde{Z}\right) - \frac{\partial^2\hat{\tilde{\Theta}}_n}{\partial\tilde{Z}^2} = 0 \qquad \text{for } \tilde{Z} > 0, \tag{33b}$$

$$\frac{\partial\hat{\tilde{\Theta}}_n}{\partial\tau} - \frac{\partial^2\hat{\tilde{\Theta}}_n}{\partial\tilde{Z}^2} = 0 \qquad \text{for } \tilde{Z} < 0 \tag{33c}$$

with boundary and matching conditions

$$\left[\hat{\tilde{\Theta}}_n\right]_-^+ = 0 \qquad \text{on } \tilde{Z} = 0, \tag{33d}$$

$$\left[\frac{\partial\hat{\tilde{\Theta}}_n}{\partial\tilde{Z}}\right]_-^+ + \alpha\left(\bar{U}_b\hat{T}_{b,n} + \bar{T}_b\hat{U}_{b,n}\right) = 0 \qquad \text{on } \tilde{Z} = 0, \tag{33e}$$

$$-\frac{\partial\hat{\tilde{\Theta}}_n}{\partial\tilde{Z}} \to \hat{\mathcal{Q}}_n \qquad \text{as } \tilde{Z} \to +\infty, \tag{33f}$$

$$\frac{\partial\hat{\tilde{\Theta}}_n}{\partial\tilde{Z}} \to 0 \qquad \text{as } \tilde{Z} \to -\infty. \tag{33g}$$

4.1.2 Solution

The perturbed biharmonic problem has solution (28j-28k), with perturbed sliding velocity and basal shear stress (28l). For the thermal problem (33) we seek a separable solution of the form

$$\left(\hat{\mathcal{Q}}_n, \hat{\tilde{\Theta}}_n\right) = \left(\hat{q}_n, \hat{\vartheta}_n\right)\exp\left(\sigma\tau\right), \quad \sigma \in \mathbb{C}. \tag{34a}$$

Direct integration of (33b-33c) with the separable ansatz above and boundary conditions (33d, 33f-33g) yields the perturbed temperature field

$$\hat{\vartheta}_n = \begin{cases} \vartheta_0\exp\left(-\tilde{Z}(ik_n\bar{U}_b + \sigma)^{1/2}\right) - \hat{q}_n\tilde{Z} & \text{for } \tilde{Z} > 0 \\ \vartheta_0\exp(\sigma^{1/2}\tilde{Z}) & \text{for } \tilde{Z} < 0 \end{cases} \tag{34b}$$

while the perturbed outer flux and perturbed basal temperature are given by the $Q-$equation (eq. 33a) and the sliding law (eq. 32c), respectively,

$$\hat{q}_n = \frac{ik_n\bar{\mathcal{Q}}\left[-2k_n + \sinh\left(2k_n\right)\right]}{ik_n\bar{U}_b + \sigma}, \quad \vartheta_0 = \frac{-2k_n\left[\bar{F}(1-\cosh\left(2k_n\right)) + \gamma\right] + \gamma\sinh\left(2k_n\right)}{\bar{T}_b F'} \tag{34c}$$

and boundedness of the temperature solution (34b) demands

$$\mathrm{Re}[\sigma^{1/2}] > 0, \quad \mathrm{Re}[(ik_n\bar{U}_b + \sigma)^{1/2}] > 0. \tag{34d}$$

Lastly, the basal energy budget (33e) yields an expression for the eigenvalue, σ, of the form

$$a_0 - a_1\left(y^2 + ik_n\bar{U}_b\right)\left[y + \left(y^2 + ik_n\bar{U}_b\right)^{1/2}\right] + a_2\left(y^2 + ik_n\bar{U}_b\right) = 0, \quad \text{with } y = \sigma^{1/2}, \tag{34e}$$

with coefficients

$$\begin{aligned} a_0 &= 2ik_n\bar{\mathcal{Q}}\left[k_n - \cosh(k_n)\sinh(k_n)\right], \\ a_1 &= \frac{-2k_n\left(\bar{F}+\gamma\right) + 2\bar{F}k_n\cosh(2k_n) + \gamma\sinh(2k_n)}{\bar{\tau}_b F'}, \\ a_2 &= -2k_n\alpha\left[\bar{\tau}_b + 2\bar{U}_b\sinh(k_n)^2\right] + \alpha\bar{\tau}_b\sinh(2k_n). \end{aligned} \tag{34f}$$

4.1.3 The roots of the dispersion relation

In order to complete the stability analysis, we need to solve eq. (34e) subject to the constraints (34d). We start by considering eq. (34e) in isolation and rearrange as

$$a_0 + \left(y^2 + ik_n\bar{U}_b\right)\left(-a_1 y + a_2\right) = a_1\left(y^2 + ik_n\bar{U}_b\right)^{3/2}. \tag{34g}$$

Squaring each side separately leads to the fifth degree polynomial in y

$$b_0 + b_1 y + b_2 y^2 + b_3 y^3 + b_4 y^4 + b_5 y^5 = 0, \tag{34h}$$

$$b_0 = a_0^2 + 2ik_n\bar{U}_b a_0 a_2 + k_n^2\bar{U}_b^2\left(-a_2^2 + ik_n\bar{U}_b a_1^2\right), \quad b_1 = -2ik_n\bar{U}_b(a_0 + ik_n\bar{U}_b a_2),$$
$$b_2 = 2\left[a_0 a_2 + ik_n\bar{U}_b\left(a_2^2 - ik_n\bar{U}_b a_1^2\right)\right], \quad b_3 = -2a_1\left(a_0 + 2ik_n\bar{U}_b a_2\right), \quad b_4 = a_2^2 - ik_n\bar{U}_b a1^2, \quad b_5 = -2a_1 a_2,$$

whose roots can be computed numerically.

Figure 2 displays solutions of eq. (34h) for a representative case. As expected for a fifth degree polynomial, we identify at most five distinct solutions. We note however that in the limits of $k_n \ll 1$ and $k_n \gg 1$ the number of distinct solutions reduces substantially: in the $k_n \gg 1$ limit, it is apparent that there are two solutions $y_{1,2}$ each with multiplicity $m_{1,2} = 2$ and such that $y_2 = -y_1$ (the yellow and red curves, and green and purple curves, respectively), while the third solution y_3 has multiplicity $m_3 = 1$ (the blue curve). The same pattern repeats for $k_n \to 0$ (see insets).

One consideration regarding the roots of eq. (34h) is that not all of them are necessarily solutions of the dispersion relation, eq. (34e). The motivation is twofold: on the one hand we might have introduced spurious solutions by squaring the two sides of eq. (34g) separately. On the other hand some solutions may not satisfy the boundedness constraints given by eq. (34d). Practically, we compute y from eq. (34h), then we check a posteriori that the computed y also satisfies eq. (34e) and the constraint eq. (34d$_1$); then compute σ through the definition eq. (34e$_2$), accounting for the multivaluedness of the square root of a complex number; last, we enforce the constraint eq. (34d$_2$).

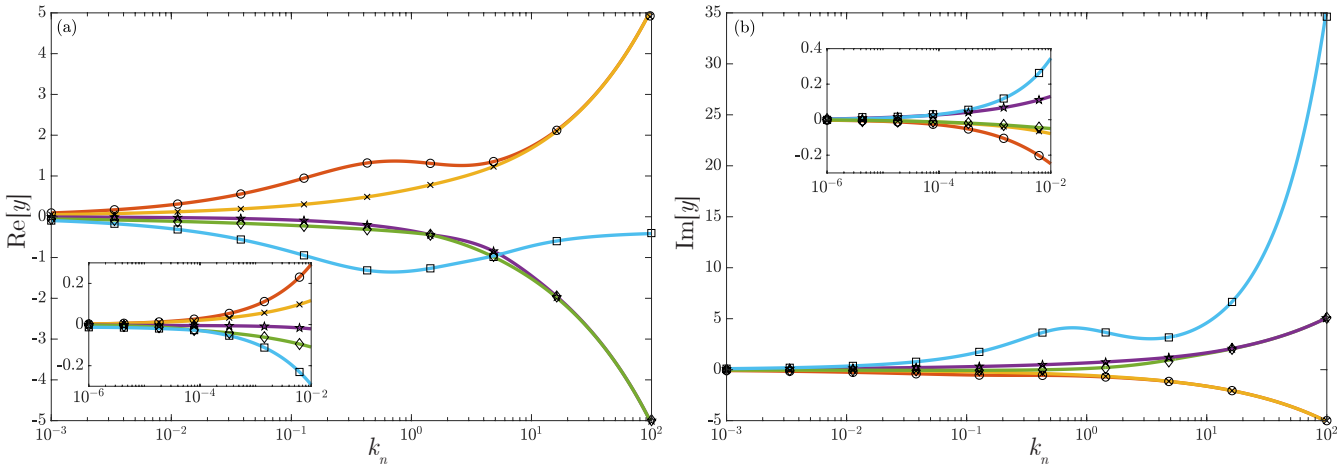

Figure 2: Real (panel a) and imaginary (panel b) part of the roots of eq. (34h) as a function of the wavenumber k_n for $\gamma = 5$ ($\bar{U}_b = 0.273$). The insets display a zoom for $k_n \to 0$. Parameters are $\nu = 1$, $\alpha = 1$, $\Theta_{bed} = -0.5$. The temperature-dependent sliding law is $F = \exp(\Theta)$.

Solutions of eq. (34e) subject to the constraints (34d) are displayed in figure 3 for three representative values of the sliding velocity (columns). The absolute value of $\mathrm{Re}[\sigma]$ as a function of k_n is displayed in the uppermost row, while the absolute value of $\mathrm{Im}[\sigma]$ is in the lowermost row. Axes are logarithmic, with colours marking different solutions; $\mathrm{Re}[\sigma], \mathrm{Im}[\sigma] > 0$ ($\mathrm{Re}[\sigma], \mathrm{Im}[\sigma] < 0$) are denoted denoted by solid (dashed) lines. To validate our numerical results, as well as to better understand the physics behind the behavior of the system, in §§4.2.1-4.2.2 we will present an asymptotic analysis for all the roots of eq. (34h). Asymptotic approximations of the solutions of the dispersion relation are displayed in light black in figure 3.

Key conclusions from our analysis are that:

1. At least one solution exists for all wavenumbers k_n, but more than one is possible for some k_n.

2. The system in unconditionally unstable for all wavenumbers, extending to $k_n \to \infty$. We will show by means of asymptotic analysis that this mode is damped in the sense of $\mathrm{Re}[\sigma] \to 0$ as $k_n^{-1/2}$ for $k_n \to \infty$, and therefore this unstable solution is well-posed.

3. Stability in the $k_n \to 0$ limit depends on the relative importance of sliding vs shearing. For slow sliding (panels a-b of fig. 3), we find an instability that extends to $k_n \to 0$ with $O(1)$ growth rate, while the growth rate $\mathrm{Re}[\sigma] \to 0$ for $k_n \to 0$ when sliding is fast (panels e-f of fig. 3).

A caveat to our analysis concerns the separation of variables approach adopted to solve the linear problem (33). This approach yields at most 5 distinct solutions; therefore the corresponding eigenfunctions fail to span the space of all possible initial conditions, which is by definition infinite-dimensional. For further insight on the stability of the system, we refer the reader to §(5) of the main text, where we present results from the numerical solution of the corresponding nonlinear problem.

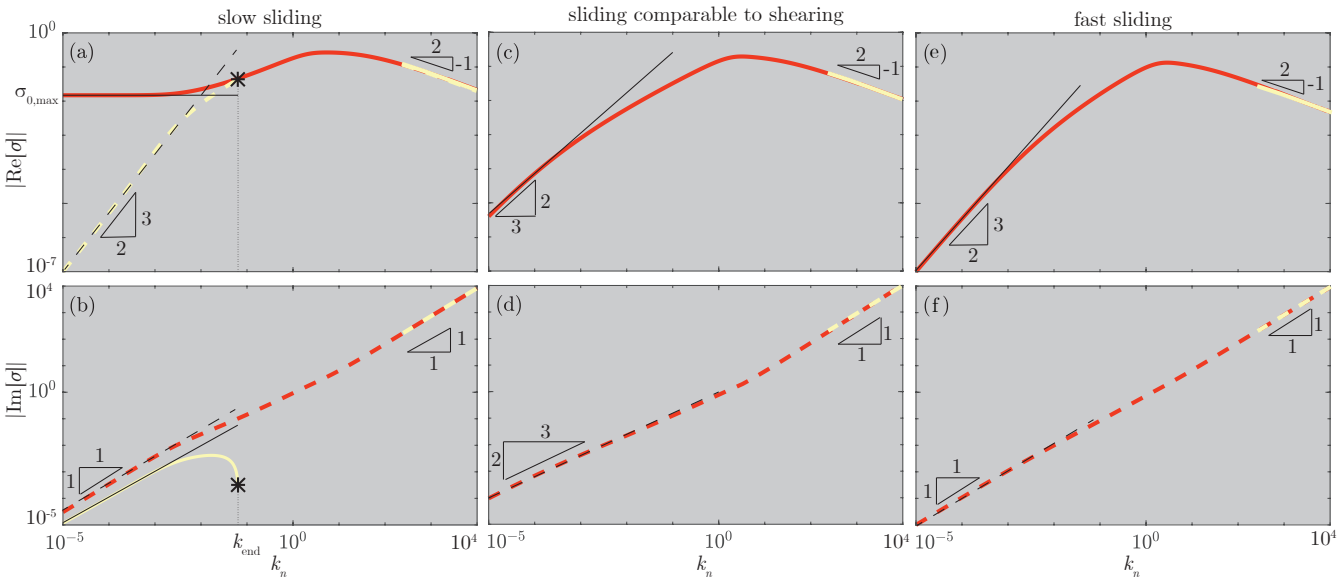

Figure 3: Numerical solution of the dispersion relation (34e) with boundedness constraints (34d) as a function of the wavenumber k_n. First (second) row displays $|\mathrm{Re}[\sigma]|$, ($|\mathrm{Im}[\sigma]|$), while columns from left to right illustrate $\bar{U}_b = (0.273, 0.5, 0.652)$. Axes are logarithmic, with colours marking different solutions; $\mathrm{Re}[\sigma], \mathrm{Im}[\sigma] > 0$ ($\mathrm{Re}[\sigma], \mathrm{Im}[\sigma] < 0$) are denoted denoted by solid (dashed) lines. Triangular shapes and numbers associated with them denote rise and run of the line best approximating the numerical solution (e.g. a rise of -1 and a run of 2 means $\sigma \sim k_n^{-1/2}$ - note that axes are logarithmic). Parameters are $\nu = 1$, $\alpha = 1$, $\Theta_{bed} = -0.5$. The temperature dependent sliding law is $F = \exp(\Theta)$.

4.2 Approximation

In this section we are concerned with an asymptotic analysis of the roots of the dispersion relation eq. (34e), with the goal to (i) derive asymptotic approximations for the eigenvalue σ in the short ($k_n \to \infty$) and long ($k_n \to 0$) wavelength limits, and (ii) confirm the numerical results presented in §4.1.3.

For the short wavelength limit, we will use the asymptotic approximation developed in §4.2.1 as a basis to derive a reduced non-linear PDE model that elucidates the physical processes governing the damping of the growth rate as $k_n \to \infty$. The interested reader is referred to §4.3.

4.2.1 Short wavelength asymptotics

We consider the limit $k_n \to \infty$, and seek a leading order approximation to the solution given by eqs. (28l, 34b-34c). Expanding in k_n, we find

$$\hat{T}_{b,n} \sim -2k_n \exp(2k_n) + O(k_n), \tag{35a}$$

$$\hat{U}_{b,n} \sim \exp(2k_n) + O(k_n), \tag{35b}$$

$$\left[\frac{\mathrm{d}\hat{\tilde{\Theta}}_n}{\mathrm{d}\hat{Z}}\right]_-^+ \sim \vartheta_0 \left[-\left(ik_n\bar{U}_b + \sigma\right)^{1/2} - \sigma^{1/2}\right] - \frac{ik_n\bar{\mathcal{Q}}\exp(2k_n)}{ik_n\bar{U}_b + \sigma} + O\left(\frac{k_n^2}{ik_n\bar{U}_b + \sigma}\right), \tag{35c}$$

$$\vartheta_0 \sim \frac{\gamma + 2k_n\bar{F}}{\bar{T}_b F'}\exp(2k_n) + O(k_n). \tag{35d}$$

Substituting into eq. (34e) and dividing by $\exp(2k_n)$ leads to

$$-\frac{\gamma + 2k_n\bar{F}}{\bar{T}_b F'}\left(ik_n\bar{U}_b + \sigma\right)\left[\left(ik_n\bar{U}_b + \sigma\right)^{1/2} + \sigma^{1/2}\right] - ik_n\bar{\mathcal{Q}} = \alpha\left(-\bar{T}_b + 2k_n\bar{U}_b\right)\left(ik_n\bar{U}_b + \sigma\right) \tag{35e}$$

which holds to leading order provided σ is not exponentially small.

In the reminder of this section we describe the two different scalings that capture the behaviour of the eigenvalue σ in the limit of $k_n \to \infty$. We anticipate that, after enforcing the constraints (34d), we will find one solution with multiplicity 2, which takes the form $\sigma \sim k_n\sigma^{(0)} + k_n^{-1/2}\sigma^{(1)}$ and has positive growth rate $\sim k_n^{-1/2}$. This is consistent with numerical results presented in figure 3 (red and yellow curves for $k_n \to \infty$), which we will discuss in more detail below.

Case 1: $\sigma \sim k_n\sigma^{(0)} + k_n^{-1/2}\sigma^{(1)}$

To find approximations for the eigenvalue, we expand $\sigma \sim k_n\sigma^{(0)} + k_n^{-1/2}\sigma^{(1)}$. To leading order eq. (35e) reduces to

$$-\frac{2k_n^{5/2}\bar{F}}{\bar{T}_b F'}\left(i\bar{U}_b + \sigma^{(0)}\right)\left[\left(i\bar{U}_b + \sigma^{(0)}\right)^{1/2} + \left(\sigma^{(0)}\right)^{1/2}\right] = 0, \tag{36a}$$

with purely imaginary solution $\sigma^{(0)} = -i\bar{U}_b$. The growth rate features at $O(k_n)$, with the dispersion relation at this order reading

$$\bar{\mathcal{Q}} \pm \frac{2\bar{F}\left(-i\bar{U}_b\right)^{1/2}\sigma^{(1)}}{\bar{T}_b F'} = 0, \tag{36b}$$

where $\pm$ accounts for the two branches of $\left(\sigma^{(0)}\right)^{1/2}$. The solution is

$$\sigma^{(1)} = \pm\frac{\bar{T}_b F'\bar{\mathcal{Q}}}{2\bar{F}\sqrt{2\bar{U}_b}}(1+i). \tag{36c}$$

Note that the term $(\sigma^{(0)})^{1/2}$ features also at second order (obtained expanding σ as $\sigma \sim k_n\sigma^{(0)} + k_n^{-1/2}\sigma^{(1)} + k_n^{-1}\sigma^{(2)}$), hence this scaling accounts effectively for 4 out of the 5 solutions of the polynomial arising from eq. (34g). These solutions are denoted by *case 1* throughout figure 4.

Next we enforce the boundedness constraints (34d). With the current scaling, these reduce to

$$\mathrm{Re}[\sigma^{1/2}] \sim \mathrm{Re}\left[\left(\sigma^{(0)}\right)^{1/2}\right] = \pm\sqrt{\bar{U}_b/2}, \tag{36d}$$

$$\mathrm{Re}[(ik_n\bar{U}_b + \sigma)^{1/2}] \sim \mathrm{Re}\left[\left(\sigma^{(1)}\right)^{1/2}\right] = \begin{cases} \left(\dfrac{\bar{T}_b F' \bar{\mathcal{Q}}}{2\bar{F}\sqrt{2\bar{U}_b}}\right)^{1/2} \sin(\pi/8) & \text{if } \left(\sigma^{(0)}\right)^{1/2} = (1-i)\sqrt{\bar{U}_b/2}, \\ -\left(\dfrac{\bar{T}_b F' \bar{\mathcal{Q}}}{2\bar{F}\sqrt{2\bar{U}_b}}\right)^{1/2} \cos(\pi/8) & \text{if } \left(\sigma^{(0)}\right)^{1/2} = -(1-i)\sqrt{\bar{U}_b/2}. \end{cases} \tag{36e}$$

Since boundedness demands that $\mathrm{Re}[\sigma^{1/2}] > 0$ and $\mathrm{Re}[(ik_n\bar{U}_b + \sigma)^{1/2}] > 0$ at the same time, we discard (36e$_2$). Accounting for the multiplicity arising at second order in σ, we conclude that this scaling yields two solutions of eq. (34e) in the short wavelength limit, of the form

$$\sigma \sim -i\bar{U}_b k_n + \frac{\bar{T}_b F' \bar{\mathcal{Q}}}{2\bar{F}\sqrt{2\bar{U}_b}}(1+i) + O(k_n^{-1}), \tag{36f}$$

both of which are linearly unstable.

These results are consistent with numerical solutions of the dispersion relation eq. (34e) with boundedness constraints 34d (figure 3). For large k_n, we find numerically two eigenvalues (red and yellow curves), which in log-log space appear to have linear $\mathrm{Re}[\sigma]$ and $\mathrm{Im}[\sigma]$, with slope $-1/2$ (uppr row), and 1 (lower row), respectively. Both solutions are unstable (solid $|\mathrm{Re}[\sigma]|$), as predicted by the asymptotics.

Case 2: $\sigma \sim k_n^2\sigma^{(0)} + k_n\sigma^{(1)}$

The former scaling accounts for 4 out of the 5 solutions of the polynomial eq. (34h). We will now show that the missing root has multiplicity $m = 1$ as expected, and behaves as $\sigma \sim k_n^2$; we will also find that this root does not satisfy the boundedness constraints (34d), hence it does not influence the dynamics.

Consider the expansions (35), and expand the eigenvalue as $\sigma \sim k_n^2\sigma^{(0)} + k_n\sigma^{(1)}$. In addition, assume $(ik_n\bar{U}_b + \sigma)^{1/2} \sim -k_n(\sigma^{(0)})^{1/2} + O(k_n^{1/2})$, which implies we are selecting the negative branch of $(ik_n\bar{U}_b + \sigma)^{1/2}$. To leading order, eq. (35e) reduces to

$$-2\alpha + \frac{i\bar{F}}{\bar{T}_b F' \left(\sigma^{(0)}\right)^{1/2}} = 0, \tag{37a}$$

with solution

$$\sigma^{(0)} = -\left(\frac{\bar{F}}{2\alpha\bar{T}_b F'}\right)^2, \tag{37b}$$

whereby we conclude that this mode is unconditionally stable. This solution is labelled as *case 2* in figure 4; we see that the numerics recover the asymptotic behaviour both as far as the sign of the growth rate is concerned (dashed line denotes $|\mathrm{Re}[\sigma]| < 0$), and in terms of dependence on k_n (see the slope of the curve in log-log coordinates).

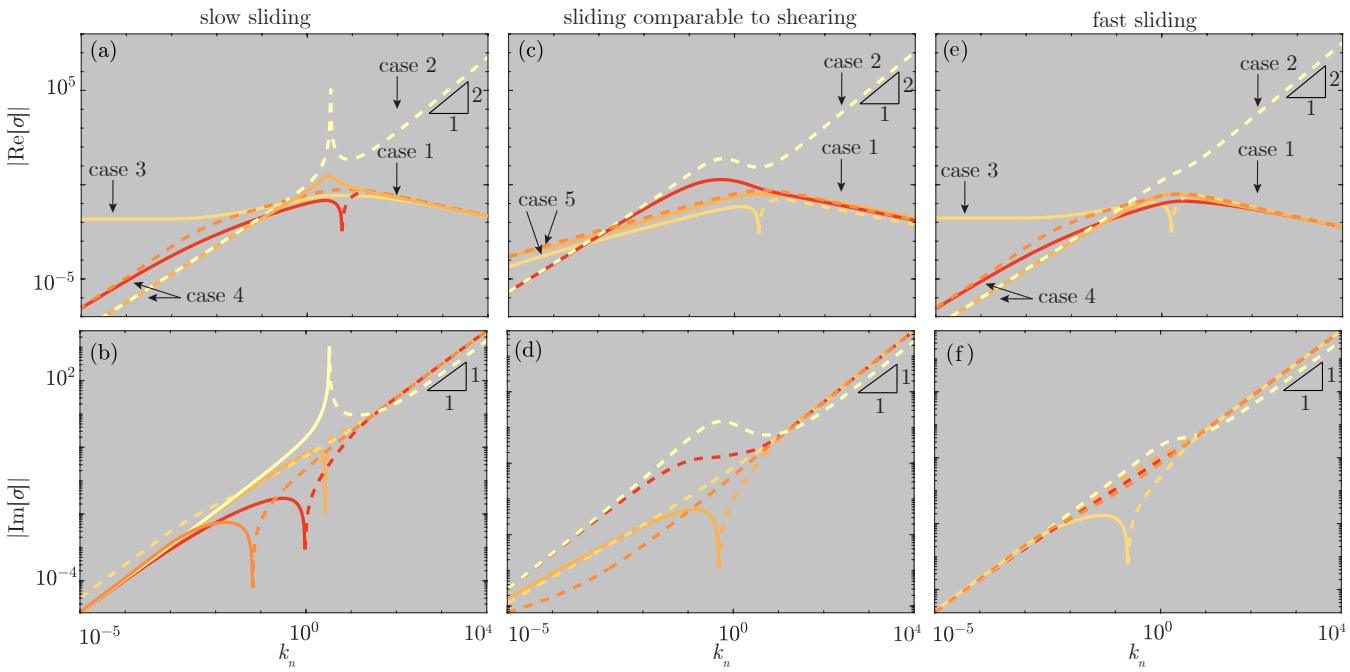

Figure 4: Same as figure 3, but without enforcing the boundedness constraints 34d. Axes are logarithmic, with colours marking different solutions; $\mathrm{Re}[\sigma], \mathrm{Im}[\sigma] > 0$ ($\mathrm{Re}[\sigma], \mathrm{Im}[\sigma] < 0$) are denoted denoted by solid (dashed) lines. The labels denoting case numbers match the various cases described in §§4.2.1-4.2.2.

Since $(\sigma^{(0)})^{1/2}$ is purely imaginary, to verify that this scaling satisfies the boundedness constraints (34d) we need to expand to higher order. From (35e) we find

$$\alpha \bar{T}_b + \frac{\bar{U}_b \left[2i\gamma\sigma^{(0)} + \bar{F}\left(\bar{U}_b - 2i\sigma^{(1)}\right)\right]}{4\bar{T}_b F' \left(\sigma^{(0)}\right)^{3/2}} = 0, \tag{37c}$$

with solution

$$\sigma^{(1)} = -\frac{i\bar{U}_b}{2} - \left(\frac{\bar{F}}{2\alpha\bar{T}_b F'}\right)^2 \left(\frac{\gamma}{\bar{F}} + \frac{\bar{T}_b}{\bar{U}_b}\right). \tag{37d}$$

An approximation of the boundedness constraints valid for $k_n \to \infty$ and $\sigma \sim k_n^2\sigma^{(0)} + k_n\sigma^{(1)}$ is

$$\mathrm{Re}[\sigma^{1/2}] \sim \mathrm{Re}\left[\frac{\sigma^{(1)}}{2\left(\sigma^{(0)}\right)^{1/2}}\right] = -\frac{\alpha\bar{T}_b\bar{U}_b F'}{2\bar{F}}, \tag{37e}$$

$$\mathrm{Re}[(ik_n\bar{U}_b + \sigma)^{1/2}] \sim \mathrm{Re}\left[\frac{\sigma^{(1)} + i\bar{U}_b}{2\left(\sigma^{(0)}\right)^{1/2}}\right] = \frac{\alpha\bar{T}_b\bar{U}_b F'}{2\bar{F}}, \tag{37f}$$

where $\alpha\bar{T}_b\bar{U}_b F'/(2\bar{F}) > 0$. Then we conclude that ($34\mathrm{d}_1$) is not satisfied, therefore this mode is never a solution to eq. (34e). This is consistent with the numerical results of figure 3, where this mode does not appear.

4.2.2 Long wavelength asymptotics

We now move to the long wavelength limit, $k_n \to 0$, and seek a leading order approximation to the solution of the linearized model, eqs. (28l, 34b-34c). Expanding in k_n, we find

$$\hat{T}_{b,n} \sim -4k_n^3 + O(k_n^5), \tag{38a}$$

$$\hat{U}_{b,n} \sim \frac{4}{3}k_n^3 + O(k_n^5), \tag{38b}$$

$$\left[-\frac{\mathrm{d}\hat{\tilde{\Theta}}_n}{\mathrm{d}\hat{Z}}\right]_-^+ \sim \vartheta_0\left[-\sigma^{1/2} - (ik_n\bar{U}_b + \sigma)^{1/2}\right] - \frac{4i\bar{\mathcal{Q}}}{3(ik_n\bar{U}_b + \sigma)}k_n^4 + O\left(k_n^5(ik_n\bar{U}_b + \sigma)^{1/2}\right) \tag{38c}$$

$$\vartheta_0 \sim \frac{4\left(3\bar{F} + \gamma\right)}{3\bar{\tau}_b F'}k_n^3 + O(k_n^5). \tag{38d}$$

Substituting into eq. (35e) and dividing by k_n^3, we find

$$\vartheta_0\left[-\sigma^{1/2} - (ik_n\bar{U}_b + \sigma)^{1/2}\right]\left(ik_n\bar{U}_b + \sigma\right) - \frac{4i\bar{\mathcal{Q}}}{3k_n} = -\alpha\left(ik_n\bar{U}_b + \sigma\right)\left(-4\bar{U}_b + \frac{4}{3}\bar{T}_b\right), \tag{38e}$$

where we have omitted terms of $O(k_n^2(ik_n\bar{U}_b + \sigma))$.

In the remainder of this section we describe the two different scalings that capture the behavior of the system in the limit of $k_n \to 0$. We anticipate that the number of actual solution to the dispersion relation after enforcing the constraints (34d) depends on the value of $\bar{U}_b$ (see figure 3), and that the case $\bar{U}_b = 1/2$ has to be treated separately.

Case 3: $\sigma \sim \sigma^{(0)} + O(k_n)$

We first seek a solution with constant growth rate, thus we pose $\sigma \sim \sigma^{(0)} + O(k_n)$. The leading order dispersion relation (33e) reduces to

$$-\frac{2\left(3\bar{F} + \gamma\right)}{3\bar{\tau}_b F'}\left(\sigma^{(0)}\right)^{1/2} + \frac{\alpha}{3}\left(-3\bar{U}_b + \bar{T}_b\right) = 0, \tag{39a}$$

with unstable solution

$$\sigma^{(0)} = \left[\frac{\alpha\bar{\tau}_b F'\left(-3\bar{U}_b + \bar{T}_b\right)}{2(3\bar{F} + \gamma)}\right]^2, \tag{39b}$$

marked as *case 3* in figure 4.

The leading order solution above is sufficient to enforce the constraints (34d). An approximation of those constraints is

$$\mathrm{Re}[\sigma^{1/2}] \sim \mathrm{Re}\left[\left(\sigma^{(0)}\right)^{1/2}\right], \quad \mathrm{Re}[(ik_n\bar{U}_b + \sigma)^{1/2}] \sim \mathrm{Re}\left[\left(\sigma^{(0)}\right)^{1/2}\right], \quad \text{for } k_n \to 0,\ \sigma \sim \sigma^{(0)} \tag{39c}$$

with

$$\left(\sigma^{(0)}\right)^{1/2} = \frac{\alpha\bar{\tau}_b F'}{2\left(3\bar{F} + \gamma\right)}\left(-3\bar{U}_b + \bar{T}_b\right). \tag{39d}$$

Both constraints are satisfied provided $-3\bar{U}_b + \bar{T}_b > 0$, or alternatively $\bar{U}_b < 1/2$. This scaling therefore accounts for one of the five possible solutions of the polynomial arising from eq. (34g) in the long wavelength limit, and it yields an unstable mode in this limit when sliding is slow, i.e., $\bar{U}_b < 1/2$.

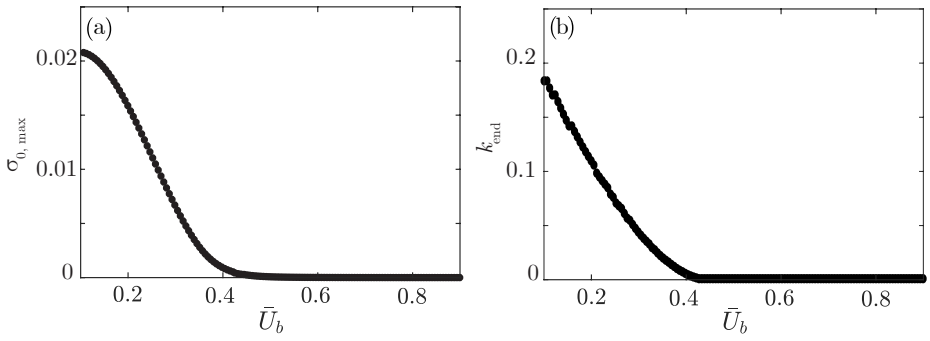

Figure 5: σ_0 and k_{end} as a function of $\bar{U}_b$. Parameters as in figure 2

Numerical results after enforcing the boundedness constraints (figure 3) are consistent with the asymptotics: a mode with constant real part $\sigma_{0,max}$ for $k_n \to 0$ is present for slow sliding (red curve in panel a), and absent for fast sliding (panel e). Panel (a) of figure (5) confirms that $\sigma_{0,max} \to 0$ as $\bar{U}_b \to 1/2$, as predicted by the asymptotics.

Physically, the instability can be understood as a feedback between frictional heating and the net heat flux into the ice: a prescribed, $O(1)$ perturbation of the basal shear stress will produce an $O(1)$ perturbation of the sliding velocity and of basal temperature that are in anti-phase with respect to the perturbed basal shear stress. With this prescribed perturbation of basal temperature, and σ real to leading order, boundedness of the temperature field then demands that the net heat flux into the ice is minimum where the bed is warmest, which further warms the bed, leading to growth of the perturbations.

Our argument so far disregards the basal energy budget; we are now going to show that it is precisely the requirement of a basal energy budget in balance that renders this mode not viable for fast sliding. To this aim, it is important to recall that a basal energy budget in balance (along with a bounded boundary layer temperature field) is possible only if the net heat flux into the ice is in anti-phase with respect to the perturbed frictional heating; the mismatch in amplitude between the two will then determine the growth rate. With perturbed basal shear stress and sliding velocity in anti-phase, and with their relative importance depending on whether sliding is slow (perturbations of the sliding velocity dominate in the frictional heating term) or fast (perturbations of the basal shear stress dominate), it is obvious that only one regime will be viable. It is straightforward to show that frictional heating is anti-phase with respect to the net heat flux into the ice for slow sliding, while it is in phase for fast sliding. This explains why this unstable mode is a solution to the linear problem for slow sliding, but it is not for fast sliding.

Case 4: $\sigma \sim k_n \sigma^{(0)} + k_n^{3/2} \sigma^{(1)}$

Numerical results illustrate the existence of a second branch of the dispersion relation for $k_n \ll 1$ (yellow curve in panels a-b of figure 3). We now seek an approximation for this branch by putting $\sigma \sim k_n \sigma^{(0)} + k_n^{3/2} \sigma^{(1)}$. To leading order the dispersion relation reads

$$\alpha \left(-3\bar{U}_b + \bar{T}_b\right) \left(i\bar{U}_b + \sigma^{(0)}\right) - i\bar{\mathcal{Q}} = 0, \tag{40a}$$

with solution

$$\sigma^{(0)} = -i\bar{U}_b + \frac{i\bar{\mathcal{Q}}}{\alpha \left(-3\bar{U}_b + \bar{T}_b\right)} \tag{40b}$$

Growth features at $O(k_n^{1/2})$, where we have a balance between ice and bed basal heat fluxes,

$$\alpha\left(-3\bar{U}_b+\bar{T}_b\right)\sigma^{(1)}-\frac{\left(3\bar{F}+\gamma\right)\left(i\bar{U}_b+\sigma^{(0)}\right)}{\bar{T}_bF'}\left[\pm\left(i\bar{U}_b+\sigma^{(0)}\right)^{1/2}\pm\left(\sigma^{(0)}\right)^{1/2}\right]=0 \tag{40c}$$

from which the first order correction ${\sigma_1}^{(1)}$ can be computed straighforwardly. In the expression above, the $\pm$ signs identify the two different branches of the square root; we thus understand that this scaling yields 4 distinct solutions of the polynomial arising from eq. (34g) before the boundedness constraints are enforced. These solutions are marked with *case 4* in figure 4.

As for the constraints (34d), an approximation valid in the long wavelength limit with this scaling is

$$\mathrm{Re}[\sigma^{1/2}]\sim\mathrm{Re}\left[\left(\sigma^{(0)}\right)^{1/2}\right]=\pm\frac{1}{2^{1/2}}\left|-\bar{U}_b+\frac{\bar{\mathcal{Q}}}{\alpha\left(-3\bar{U}_b+\bar{T}_b\right)}\right|^{1/2}, \tag{40d}$$

$$\mathrm{Re}[(ik_n\bar{U}_b+\sigma)^{1/2}]\sim\mathrm{Re}\left[\left(i\bar{U}_b+\sigma^{(0)}\right)^{1/2}\right]=\pm\frac{1}{2^{1/2}}\left|\frac{\bar{\mathcal{Q}}}{\alpha\left(-3\bar{U}_b+\bar{T}_b\right)}\right|^{1/2}, \tag{40e}$$

so we have one solution of eq. (34*e*) that derives from the positive branches of both $\sigma^{1/2}$ and $(\sigma+ik_n\bar{U}_b)^{1/2}$.

Physically, this mode corresponds to a travelling wave such that $O(1)$ changes in frictional heating (either through basal shear stress or sliding velocity) cause $O(1)$ changes in the outer flux, $\mathcal{Q}'$. This is accommodated by a small ($\sim O(k_n^{1/2})$) perturbation of basal temperature which can be stable or unstable. Regardless of the parameter regime, the asymptotics predict that this branch is damped, in the sense of $\mathrm{Re}[\sigma]\to 0$ for $k_n\to 0$. This is confirmed by numerical results (panels a,f of figure 3), which also illustrate that this mode is unstable for $\bar{U}_b>1/2$ and stable otherwise.

A last consideration is that this branch of the dispersion relation spans a finite bandwidth, at least in certain parameter regimes. This is illustrated in panels (a-b) of figure 3, where the end of the branch at $k_n=k_{end}$ is marked with a star. We find numerically (panel b of figure 5) that $k_{end}\to 0$ as $\bar{U}_b\to 1/2$; this also corresponds to a transition from stability ($\bar{U}_b<1/2$) to instability ($\bar{U}_b>1/2$) of this branch.

Case 5: long wavelength limit for $\bar{U}_b=1/2$

The scalings for cases 1 and 2 no longer work when $\bar{T}_b=3\bar{U}_b$ (or equivalently $\bar{U}_b=1/2$), as a result of the perturbation of frictional heating becoming small ($\sim O(k_n^5)$). For brevity, here we discuss only the scaling that explains the numerical results presented in figure 3 (panels c-d), which we can approximate by expanding $\sigma\sim k_n^{2/3}\sigma^{(0)}$.

Substituting into the dispersion relation, to leading order we find

$$-i\bar{\mathcal{Q}}+\left[-\frac{2(3\bar{F}+\gamma)}{\bar{T}_bF'}\left(\sigma^{(0)}\right)^{3/2}\right]=0, \tag{41a}$$

with solutions

$$\begin{aligned}
{\sigma_1}^{(0)}&=\left(\frac{\bar{T}_bF'\bar{\mathcal{Q}}}{2(3\bar{F}+\gamma)}\right)^{2/3}\frac{(1+\sqrt{3}i)}{2} \quad \text{if } \left(\sigma^{(0)}\right)^{1/2}=\Sigma_-,\\
{\sigma_2}^{(0)}=\left(\frac{\bar{T}_bF'\bar{\mathcal{Q}}}{2(3\bar{F}+\gamma)}\right)^{2/3}\frac{(1-\sqrt{3}i)}{2},\quad {\sigma_3}^{(0)}&=-\left(\frac{\bar{T}_bF'\bar{\mathcal{Q}}}{2(3\bar{F}+\gamma)}\right)^{2/3} \quad \text{if } \left(\sigma^{(0)}\right)^{1/2}=\Sigma_+,
\end{aligned} \tag{41b}$$

where Σ_+ and Σ_- indicate respectively the positive and negative branch of $\left(\sigma^{(0)}\right)^{1/2}$. These three solutions are marked as *case 5* in figure 4 (panels c-d).

As far as the boundedness constraints (34d) are concerned, we recognize that in this limit

$$\mathrm{Re}[\sigma^{1/2}] \sim \mathrm{Re}\left[\left(\sigma^{(0)}\right)^{1/2}\right], \quad \mathrm{Re}[(ik_n\bar{U}_b+\sigma)^{1/2}] \sim \mathrm{Re}\left[\left(\sigma^{(0)}\right)^{1/2}\right]. \tag{41c}$$

Selecting branches of the square root consistently with (41b), we find

$$\left(\sigma^{(0)}{}_1\right)^{1/2} = -\left(\frac{\bar{T}_b F'\bar{\mathcal{Q}}}{2(3\bar{F}+\gamma)}\right)^{1/3}\frac{(\sqrt{3}+i)}{2}, \quad \left(\sigma^{(0)}{}_2\right)^{1/2} = \left(\frac{\bar{T}_b F'\bar{\mathcal{Q}}}{2(3\bar{F}+\gamma)}\right)^{1/3}\frac{(\sqrt{3}-i)}{2}, \tag{41d}$$

so we discard σ_1. As for σ_3, $\left(\sigma_3{}^{(0)}\right)^{1/2}$ is purely imaginary, so we expand to higher order to find $\sigma_3{}^{(1)} = -5i\bar{U}_b/6$. An approximation of the boundedness constraints in this case is

$$\mathrm{Re}[\sigma^{1/2}] \sim \mathrm{Re}\left[\frac{\sigma^{(1)}}{2\left(\sigma^{(0)}\right)^{1/2}}\right] = -\frac{5\bar{U}_b}{12|\sigma_3{}^{(0)}|^{1/2}}, \tag{41e}$$

$$\mathrm{Re}[(ik_n\bar{U}_b+\sigma)^{1/2}] \sim \mathrm{Re}\left[\frac{\sigma^{(1)}+i\bar{U}_b}{2\left(\sigma^{(0)}\right)^{1/2}}\right] \sim \frac{\bar{U}_b}{12|\sigma_3{}^{(0)}|^{1/2}}, \tag{41f}$$

whereby we conclude that σ_3 is not a solution either. We are therefore left with σ_2, consistently with our numerical results (3, panels c-d) that illustrate $\mathrm{Re}[\sigma], \mathrm{Im}[\sigma] \sim k_n^{2/3}$, with $\mathrm{Re}[\sigma] > 0$ and $\mathrm{Im}[\sigma] < 0$.

4.3 A non-linear model in the short wavelength limit, $k_n \to +\infty$

In this section we seek to derive a leading order version of the ice thickness scale model with finite δ described in §2.3.1 that holds in the limit of a short horizontal length scale.

In order to streamline notation, take (x, z) as the ice thickness scale horizontal and vertical coordinates, t as the fast time scale considered in model of §2.3.1, (u, w) as the ice thickness scale velocity field, p as the first order pressure fiels, Q as the outer basal heat flux, Z as the boundary layer vertical coordinate, and θ as the boundary layer temperature. Then the leading order problem at the ice thickness scale can be rewritten as

$$\nabla^2\boldsymbol{u} - \nabla p + \boldsymbol{i} = \boldsymbol{0}, \tag{42a}$$

$$\nabla\cdot\boldsymbol{u} = 0 \tag{42b}$$

for $0 < z < 1$, with $\boldsymbol{u} = (u, w)$ and $\nabla = (_x, _z)$, and

$$w = \frac{\partial u}{\partial z} + \frac{\partial w}{\partial x} = 0 \qquad \text{on } z = 1, \tag{42c}$$

$$w = 0 \qquad \text{on } z = 0, \tag{42d}$$

$$u = \gamma^{-1}F(Pe^{-1/2}\varepsilon^{1/2}\delta^{-1}\theta)\left(\frac{\partial u}{\partial z} + \frac{\partial w}{\partial x}\right) \qquad \text{on } z = Z = 0, \tag{42e}$$

as well as

$$\frac{\partial\theta}{\partial t} + u_b\frac{\partial\theta}{\partial x} - \frac{\partial u_b}{\partial x}Z\frac{\partial\theta}{\partial Z} - \frac{\partial^2\theta}{\partial Z^2} = 0 \qquad \text{for } Z > 0, \tag{42f}$$

$$\frac{\partial\theta}{\partial t} - \frac{\partial^2\theta}{\partial Z^2} = 0 \qquad \text{for } Z < 0, \tag{42g}$$

and

$$-\frac{\partial\theta}{\partial Z} \to Q \qquad \text{as } Z \to \infty \tag{42h}$$

$$-\frac{\partial\theta}{\partial Z} \to \nu \qquad \text{as } Z \to -\infty \tag{42i}$$

$$\left[-\frac{\partial\theta}{\partial Z}\right]_-^+ = \alpha u_b \tau_b \qquad \text{on } Z = 0, \tag{42j}$$

$$[\theta]_-^+ = 0 \qquad \text{on } Z = 0, \tag{42k}$$

where

$$u_b = u|_{z=0}, \qquad \tau_b = \left(\frac{\partial u}{\partial z} + \frac{\partial w}{\partial x}\right)\bigg|_{z=0}. \tag{42l}$$

and

$$\frac{\partial Q}{\partial t} + u_b \frac{\partial Q}{\partial x} = Q \frac{\partial u_b}{\partial x}. \tag{42m}$$

As usual, $[\cdot]_-^+$ denotes the difference between limiting values taken as $Z = 0$ is approached from above and below.

Let k^{-1} be a length scale, with $k \gg 1$. Based on the results of the stability analysis, rescale the problem as

$$x = k^{-1}\tilde{x}, \qquad z = k^{-1}\tilde{z}, \qquad t = k^{-1}T = k^{1/2}\tilde{t}, \qquad \boldsymbol{u} = \tilde{\boldsymbol{u}}, \qquad p = k^{-1/2}\tilde{p}, \qquad u_b = \tilde{u}_b, \qquad \tau_b = \tilde{\tau}_b$$

$$\theta = \tilde{\theta}, \qquad Z = k^{-1/2}\tilde{Z}, \qquad Q = \tilde{Q}. \tag{43a}$$

Note that we have multiply-scaled time variables T and $\tilde{t}$, and will treat the problem as a multiple scales expansion.

In addition, expand as

$$\tilde{\boldsymbol{u}} = \tilde{u}_b^{(0)}\boldsymbol{i} + k^{-1}\tilde{z}\boldsymbol{i} + k^{-3/2}\tilde{\boldsymbol{u}}^{(1)} + o(k^{-3/2}), \qquad \tilde{u}_b = \tilde{u}_b^{(0)} + k^{-3/2}u_b^{(1)},$$

$$\tilde{\tau}_b = \tilde{\tau}_b^{(0)} + k^{-1/2}\tilde{\tau}_b^{(1)}, \qquad \tilde{\theta} = \tilde{\theta}^{(0)} + k^{-1/2}\tilde{\theta}^{(1)}, \qquad \tilde{Q} = \tilde{Q}^{(0)} + k^{-3/2}\tilde{Q}^{(1)}, \tag{43b}$$

with $\tilde{u}_b^{(0)}$, $\tilde{\tau}_b^{(0)}$ and $\tilde{\theta}^{(0)}$ dependent on $\tilde{t}$ only (that is, independent of $\tilde{x}$, $\tilde{Z}$ and T).

We develop expansions only to the order required to construct a closed model for the zeroth-order flux $Q^{(0)}$ as a function of the inner and outer time variables, T and $\tilde{t}$. We have

$$\tilde{\nabla}^2\tilde{\boldsymbol{u}}^{(1)} - \tilde{\nabla}\tilde{p} = \boldsymbol{0}, \tag{44a}$$

$$\tilde{\nabla}\cdot\tilde{\boldsymbol{u}}^{(1)} = 0 \tag{44b}$$

for $0 < \tilde{z}$, with $\tilde{\boldsymbol{u}}^{(1)} = (\tilde{u}^{(1)}, \tilde{w}^{(1)})$ and $\tilde{\nabla} = (_{\tilde{x}}, _{\tilde{z}})$, and

$$\tilde{w}^{(1)} = 0 \qquad \text{on } \tilde{z} = 0, \tag{44c}$$

$$\tilde{u}_b^{(0)} + O(k^{-3/2}) = \gamma^{-1}F\left[Pe^{-1/2}\delta^{-1}\left(\tilde{\theta}^{(0)} + k^{-1/2}\tilde{\theta}^{(1)}\right)\right]\left(\tilde{\tau}_b^{(0)} + k^{-1/2}\tilde{\tau}_b^{(1)}\right) \quad \text{on } \tilde{z} = \tilde{Z} = 0 \tag{44d}$$

where

$$\tilde{\tau}_b^{(0)} = 1, \qquad \tilde{\tau}_b^{(1)} = \left(\frac{\partial\tilde{u}^{(1)}}{\partial\tilde{z}} + \frac{\partial\tilde{w}^{(1)}}{\partial\tilde{z}}\right)\bigg|_{\tilde{z}=0}, \qquad \tilde{u}_b^{(1)} = \tilde{u}^{(1)}\big|_{\tilde{z}=0}. \tag{44e}$$

The rescaling renders the flow problem in the form of a boundary layer, occupying a half space domain, and the appropriate boundary conditions as $\tilde{z} \to \infty$ are that $\tilde{\boldsymbol{u}}^{(1)} \to 0$.

In addition,

$$\frac{\partial \tilde{\theta}^{(1)}}{\partial T} + \tilde{u}_b^{(0)} \frac{\partial \tilde{\theta}^{(1)}}{\partial \tilde{x}} - \frac{\partial^2 \tilde{\theta}^{(1)}}{\partial \tilde{Z}^2} = O(k^{3/2}) \qquad \text{for } \tilde{Z} > 0, \tag{44f}$$

$$\frac{\partial \tilde{\theta}^{(1)}}{\partial T} - \frac{\partial^2 \tilde{\theta}^{(1)}}{\partial \tilde{Z}^2} = O(k^{3/2}) \qquad \text{for } \tilde{Z} < 0, \tag{44g}$$

and

$$-\frac{\partial \tilde{\theta}^{(1)}}{\partial \tilde{Z}} \to \tilde{Q} \qquad \text{as } \tilde{Z} \to \infty \tag{44h}$$

$$-\frac{\partial \tilde{\theta}^{(1)}}{\partial \tilde{Z}} \to \nu \qquad \text{as } \tilde{Z} \to -\infty \tag{44i}$$

$$\left[-\frac{\partial \tilde{\theta}^{(1)}}{\partial \tilde{Z}} \right]_-^+ = \alpha \tilde{u}_b^{(0)} \tilde{\tau}_b^{(0)} + O(k^{-1/2}) \qquad \text{on } \tilde{Z} = 0, \tag{44j}$$

and

$$\frac{\partial \tilde{Q}^{(0)}}{\partial T} + k^{-3/2} \frac{\partial \tilde{Q}^{(0)}}{\partial \tilde{t}} + k^{-3/2} \frac{\partial \tilde{Q}^{(1)}}{\partial T} + \left(\tilde{u}_b^{(0)} + k^{-3/2} u_b^{(1)} \right) \left(\frac{\partial \tilde{Q}^{(0)}}{\partial \tilde{x}} + k^{-3/2} \frac{\partial \tilde{Q}^{(1)}}{\partial \tilde{x}} \right) = k^{-3/2} \tilde{Q}^{(0)} \frac{\partial \tilde{u}_b^{(1)}}{\partial \tilde{x}} + o(k^{3/2}). \tag{44k}$$

Clearly, $\tilde{u}_b^{(0)}$ and $\tilde{\theta}^{(0)}$ are related through

$$u_b^{(0)} = F\left[Pe^{-1/2} \varepsilon^{1/2} \delta^{-1} \tilde{\theta}^{(0)} \right];$$

we will later be able to relate $\tilde{u}_b^{(0)}$ to $\tilde{Q}^{(0)}$. In addition, we obtain (44a)–(44c) with

$$\left(\frac{\partial \tilde{u}^{(1)}}{\partial \tilde{z}} + \frac{\partial \tilde{w}^{(1)}}{\partial \tilde{z}} \right) = -\, c\left(\tilde{u}_b^{(0)}, \tilde{\theta}^{(0)} \right) \tilde{\theta}^{(1)} \qquad \text{on } \tilde{z} = \tilde{Z} = 0. \tag{45a}$$

where

$$c(\tilde{u}_b^{(0)}, \tilde{\theta}^{(0)}) = \frac{Pe^{-1/2} \varepsilon^{1/2} \delta^{-1} F'\left(Pe^{-1/2} \varepsilon^{1/2} \delta^{-1} \tilde{\theta}^{(0)} \right)}{F\left(Pe^{-1/2} \varepsilon^{1/2} \delta^{-1} \tilde{\theta}^{(0)} \right)}. \tag{45b}$$

As before, $\tilde{\boldsymbol{u}}^{(1)} \to \mathbf{0}$ as $\tilde{z} \to \infty$.

Meanwhile, the temperature problem in the ice ($\tilde{Z} > 0$) has the simple linear-in-$\tilde{Z}$ solution

$$\tilde{\theta}^{(1)}(\tilde{x}, \tilde{Z}, T, \tilde{t}) = \tilde{\theta}_0^{(1)}(\tilde{x}, T, \tilde{t}) - \tilde{Q}^{(0)}(\tilde{x}, T, \tilde{t}) \tilde{Z}, \tag{45c}$$

where $\theta_0 = \tilde{\theta}^{(1)}\Big|_{\tilde{Z}=0}$ and the flux $\tilde{Q}^{(0)}$ satisfy the standard first-order linear advection problem

$$\frac{\partial \tilde{\theta}_0^{(1)}}{\partial T} + \tilde{u}_b^{(0)} \frac{\partial \tilde{\theta}_0^{(1)}}{\partial \tilde{x}} = 0. \tag{45d}$$

$$\frac{\partial \tilde{Q}^{(0)}}{\partial T} + \tilde{u}_b^{(0)} \frac{\partial \tilde{Q}^{(0)}}{\partial \tilde{x}} = 0. \tag{45e}$$

where $\tilde{u}_b^{(0)}$ depends on $\tilde{t}$ only, so that

$$\tilde{\theta}_0^{(1)}(\tilde{x},T,\tilde{t}) = \theta_0(\tilde{x}-\tilde{u}_b^{(0)}(\tilde{t})T,\tilde{t}), \tag{45f}$$

$$\tilde{Q}^{(0)}(\tilde{x},T,\tilde{t}) = Q_0(\tilde{x}-\tilde{u}_b^{(0)}(\tilde{t})T,\tilde{t}) \tag{45g}$$

where θ_0 and Q_0 are functions to be determined. That this works (in the sense of the diffusion term in (44f) being irrelevant) is the result of such a solution being compatible with the one-dimensional diffusion problem (44g) in the bed. The temperature θ_0 at the ice-bed interface $\tilde{Z}=0$ is in fact determined by

$$\frac{\partial\tilde{\theta}^{(1)}}{\partial\tilde{t}} - \frac{\partial^2\tilde{\theta}^{(1)}}{\partial\tilde{Z}^2} = 0 \qquad \text{for } \tilde{Z}<0, \tag{45h}$$

$$-\frac{\partial\tilde{\theta}^{(1)}}{\partial\tilde{Z}} \to \nu \qquad \text{as } \tilde{Z}\to-\infty, \tag{45i}$$

$$\tilde{Q}^{(0)} = \alpha\tilde{u}_b^{(0)} - \lim_{\tilde{Z}\to0^-}\frac{\partial\tilde{\theta}^{(1)}}{\partial\tilde{Z}}, \tag{45j}$$

$$\tilde{\theta}_0^{(1)} = \lim_{\tilde{Z}\to0^-}\tilde{\theta}^{(1)} \tag{45k}$$

and $\theta_0^{(1)}$ feeds back into the determination of the perturbed velocity field $u_b^{(1)}$ through (45a) above. Recall once more that $\tilde{u}_b^{(0)}$ is independent of the inner variables $\tilde{x}$ and T.

For simplicity, assume that the domain is periodic in $\tilde{x}$ with period L. A large-T solution for $\tilde{\theta}^{(1)}$ can then be found using a Fourier series in $\tilde{x}$, defining

$$\hat{f}_n(\tilde{Z},T,\tilde{\tau}) = \frac{1}{L}\int_0^L \tilde{f}(\tilde{x},\tilde{Z},T,\tilde{\tau})\exp(-ik_nX)\mathrm{d}\tilde{x}, \qquad k_n = \frac{2\pi n}{L}.$$

Then

$$\hat{\theta}_0^{(1)} = -\nu\tilde{Z}, \tag{45l}$$

$$\hat{\theta}_n^{(1)} = -\frac{\hat{Q}_{0,n}}{(1-i)\sqrt{|k_n|\hat{u}_b^{(0)}/2}}\exp\left(\sqrt{\frac{|k_n|\hat{u}_b^{(0)}}{2}}(1-i)\tilde{Z} - ik_n\hat{u}_b^{(0)}T\right), \qquad n\neq0 \tag{45m}$$

where $\hat{Q}_{0,n} = a^{-1}\int_0^a Q_0(\tilde{x},\tilde{\tau})\exp(-ik_n\tilde{x})\mathrm{d}\tilde{x}$ is the Fourier transform of the travelling wave far field flux pattern. To satisfy the flux boundary condition at $\tilde{Z}=0$ with $n=0$, we further require the energy balance constraint

$$\nu = \frac{1}{L}\int_0^L Q_0(\tilde{x},\tilde{\tau})\mathrm{d}\tilde{x} - \alpha\tilde{u}_b^{(0)}(\tilde{\tau}), \tag{45n}$$

to be satisfied, which defines $\tilde{u}_b^{(0)}$ in terms of the flux.

The temperature perturbation $\tilde{\theta}^{(1)}$ at the interface $\tilde{Z}=0$, which determines the perturbed ice velocity through (45a), can therefore be found linearly in terms of the flux $\tilde{Q}^{(0)}$; in terms of Fourier coefficients

$$\hat{\theta}_{0,n}^{(1)} = -\frac{\hat{Q}_n^{(0)}}{(1-i)\sqrt{|k_n|\hat{u}_b^{(0)}/2}}. \tag{45o}$$

We can finally use this to relate the velocity perturbation $\tilde{u}_b^{(1)}$ to the flux $\tilde{Q}^{(0)}$. By using the same Fourier transform convention as above, we can show that

$$\hat{u}_{b,n}^{(1)} = -\frac{\hat{\tau}_{b,n}^{(1)}}{2|k_n|} = \frac{c_1\left(\tilde{u}_b^{(0)}, \tilde{\theta}^{(0)}\right)}{2}|k_n|^{-1}\hat{\theta}_{0,n}^{(1)} = \frac{c_1\left(\tilde{u}_b^{(0)}, \tilde{\theta}^{(0)}\right)}{\sqrt{2\tilde{u}_b^{(0)}}}\frac{\hat{Q}_n^{(0)}}{(1-i)|k_n|^{3/2}} \tag{45p}$$

so the velocity pattern $\tilde{u}_b^{(1)}$ is related to the flux $\tilde{Q}^{(0)}$ through a convolution integral through a convolution integral

$$\tilde{u}_b^{(1)}(\tilde{x},\tilde{t}) = \frac{1}{L}\int_0^L G(\tilde{x}-\tilde{x}')\tilde{Q}^{(0)}(\tilde{x}',T,\tilde{t})\mathrm{d}\tilde{x}' \tag{45q}$$

where

$$G(x) = \frac{c_1\left(\tilde{u}_b^{(0)}, \tilde{\theta}^{(0)}\right)}{\sqrt{2\tilde{u}_b^{(0)}}}\sum_{n=-\infty, n\neq=0}^{\infty}\frac{1}{(1-i)|k_n|^{3/2}}$$

The model thus far is purely linear and consists of the diffusive propagation of a travelling wave heat flux signal into the bed. Temperature in the bed has a simple travelling-wave-in-$\tilde{x}$ solution that attenuates and gathers a phase shift as $\tilde{Z}$ becomes more negative (i.e., with distance below the bed). This results in an interface temperature $\tilde{\theta}^{(1)}$ that is phase shifted relative to the imposed flux (in fact, for a single Fourier mode, temperature lags flux by 1/4 of a cycle). The sliding law, having to maintain a constant leading order sliding velocity, therefore results in basal shear stress perturbation $\tilde{\tau}_b^{(1)}$, and a sliding velocity perturbation $\tilde{u}_b^{(1)}$ that is similarly phase shifted. In fact, the sliding velocity lags flux by 1/4 of a cycle, so, again for a single mode, $\tilde{u}_{b,x}^{(1)}$ is positive where $\tilde{Q}_0^{(1)}$ has a maximum. This is key to driving the instability at the slow time scale.

Growth occurs at the slow time scale associated with $\tilde{t}$, and is driven by the effect of that velocity perturbation on the flux $Q^{(0)}$. Taking the Q-equation (44k) at $O(k^{-3/2})$,

$$\frac{\partial\tilde{Q}^{(1)}}{\partial T} + \tilde{u}_b^{(0)}\frac{\partial\tilde{Q}^{(1)}}{\partial\tilde{x}} + \left[\frac{\partial\tilde{Q}^{(0)}}{\partial\tilde{t}} + \tilde{u}_b^{(1)}\frac{\partial\tilde{Q}^{(0)}}{\partial\tilde{x}} - \tilde{Q}^{(0)}\frac{\partial\tilde{u}_b^{(1)}}{\partial\tilde{x}}\right] = 0. \tag{45r}$$

$\tilde{Q}^{(1)}$ satisfies the same linear advection problem as $\tilde{Q}^{(0)}$, but with an inhomogeneous term. In the usual manner of multiple scales problems, we can close the problem for $\tilde{Q}^{(0)}$ by demanding that the inhomogeneous term should not lead to secular growth of the first order correction $\tilde{Q}^{(1)}$.

This is easy to do; the natural first step is to switch to characteristic coordinates defined through

$$\sigma = \tilde{x} - \tilde{u}_b^{(0)}T, \qquad \tau = T, \tag{45s}$$

so that

$$\frac{\partial\tilde{Q}^{(1)}}{\partial\tau} + \left[\frac{\partial\tilde{Q}^{(0)}}{\partial\tilde{t}} + \tilde{u}_b^{(1)}\frac{\partial\tilde{Q}^{(0)}}{\partial\sigma} - \tilde{Q}^{(0)}\frac{\partial\tilde{u}_b^{(1)}}{\partial\sigma}\right] = 0, \tag{45t}$$

treating $\tilde{Q}^{(0)}$, $\tilde{Q}^{(1)}$ and $\tilde{u}_b^{(1)}$ as functions of τ, σ and $\tilde{t}$ instead of $\tilde{x}$, T and $\tilde{t}$ to avoid more excessive notation.

Recall that $\tilde{Q}^{(0)}$ and hence, through the solution of the bed temperature and ice flow problems, $\tilde{u}_b^{(1)}$ are functions of σ but not τ. Keeping $\tilde{Q}^{(1)}$ bounded then requires that the inhomogeneous term in (45t) should vanish, so

$$\frac{\partial\tilde{Q}^{(0)}}{\partial\tilde{t}} + \tilde{u}_b^{(1)}\frac{\partial\tilde{Q}^{(0)}}{\partial\sigma} - \tilde{Q}^{(0)}\frac{\partial\tilde{u}_b^{(1)}}{\partial\sigma} = 0. \tag{45u}$$

This closes the nonlinear problem for the evolution of $\tilde{Q}^{(0)}$ on the slow time scale. Growth of perturbations away from the trivial solution $\tilde{Q}^{(0)} =$ constant is caused by the third term, which is proportional to the divergence of the perturbed basal velocity. As discussed before, this is positive where $\tilde{Q}^{(0)}$ has a maximum, thus driving growth for small perturbations in $\tilde{Q}^{(0)}$. Numerical solutions of eqs. (42) demonstrates that perturbations grow unboundedly till portions of the bed freeze, at which point the simple advection-diffusion model in the ice, eq. (42f), fails because u_b is no longer $O(1)$. For further detail, the reader is referred to §5 of the main text.

5 Stability at longer length scales with $\delta \sim \varepsilon^{1/2}$

5.1 Stability of the intermediate scale model

5.1.1 Linearized model

We are concerned with the stability of the model (25g-25u) to small amplitude perturbations. To this aim, assume a periodic domain of length L, and we expand dependent variables as

$$\mathsf{h}^{(0)} = \bar{\mathsf{h}}, \quad \mathsf{h}^{(1)} = \beta \mathsf{h}', \quad {\mathsf{u}_b}^{(0)} = \bar{\mathsf{u}_b} + \beta \mathsf{u}_b', \quad {\mathsf{t}_b}^{(0)} = \bar{\mathsf{t}_b} + \beta \mathsf{t}_b', \quad \tilde{\mathsf{T}}^{(0)} = \bar{\tilde{\mathsf{T}}} + \beta \tilde{\mathsf{T}}', \quad \beta \ll 1 \tag{46a}$$

where barred quantities are independent of x, τ, while we Fourier-transform perturbed variables in x as

$$\hat{\mathsf{g}}_n = \frac{1}{L} \int_0^L \mathsf{g}' \exp\left(-ik\mathsf{x}\right) \mathrm{d}\mathsf{x}, \quad k = \frac{2\pi n}{L} \tag{46b}$$

and we also assume separation of variable, so that $\partial \hat{\mathsf{g}}_n / \partial \tau = \sigma \hat{\mathsf{g}}_n$. Substituting into the governing equations and linearizing, we find the following $O(\beta)$ problem

$$\sigma \hat{\mathsf{h}}_n + ik_n \bar{\mathsf{h}}_n \hat{\mathsf{U}}_{b,n} + k_n^2 \frac{\bar{\mathsf{h}}_n^3}{3} \hat{\mathsf{h}}_n = 0, \tag{46c}$$

with

$$\hat{\mathsf{U}}_{b,n} = \gamma^{-1} \left(\bar{F} \hat{\mathsf{t}}_{b,n} + \bar{\mathsf{t}}_b F' \hat{\tilde{\mathsf{T}}}_n \right), \quad \hat{\mathsf{t}}_{b,n} = -ik_n \bar{\mathsf{h}} \hat{\mathsf{h}}_n, \tag{46d}$$

and $F' = \mathrm{d}F/\mathrm{d}\mathsf{T}|_{\bar{\mathsf{T}}}$ for evaluated on $\mathsf{z} = 0$. The heat equation simplifies to

$$\sigma \hat{\tilde{\mathsf{T}}}_n - \frac{\mathrm{d}^2 \hat{\tilde{\mathsf{T}}}_n}{\mathrm{d}\tilde{\mathsf{z}}^2} = 0, \quad \text{for} \quad -\infty < \tilde{\mathsf{z}} < +\infty, \tag{46e}$$

with boundary conditions

$$\frac{\mathrm{d}\hat{\tilde{\mathsf{T}}}_n}{\mathrm{d}\tilde{\mathsf{z}}} \to 0 \quad \text{as } \tilde{\mathsf{z}} \to \pm\infty, \tag{46f}$$

$$\left[\frac{\mathrm{d}\hat{\tilde{\mathsf{T}}}_n}{\mathrm{d}\tilde{\mathsf{z}}} \right]_-^+ + \alpha \left(\bar{\mathsf{t}}_b \hat{\mathsf{U}}_{b,n} + \bar{\mathsf{U}}_b \hat{\mathsf{t}}_{b,n} \right) = 0 \quad \text{on } \tilde{\mathsf{z}} = 0. \tag{46g}$$

5.1.2 Solution

The heat equation (46e) can be integrated straightforwardly along with (46f) yielding

$$\hat{\tilde{\mathsf{T}}}_n = \begin{cases} \mathsf{T}_0 \exp\left(-\tilde{\mathsf{z}}\sigma^{1/2}\right) & \text{for } \tilde{\mathsf{z}} > 0 \\ \mathsf{T}_0 \exp\left(\tilde{\mathsf{z}}\sigma^{1/2}\right) & \text{for } \tilde{\mathsf{z}} < 0 \end{cases} \tag{47a}$$

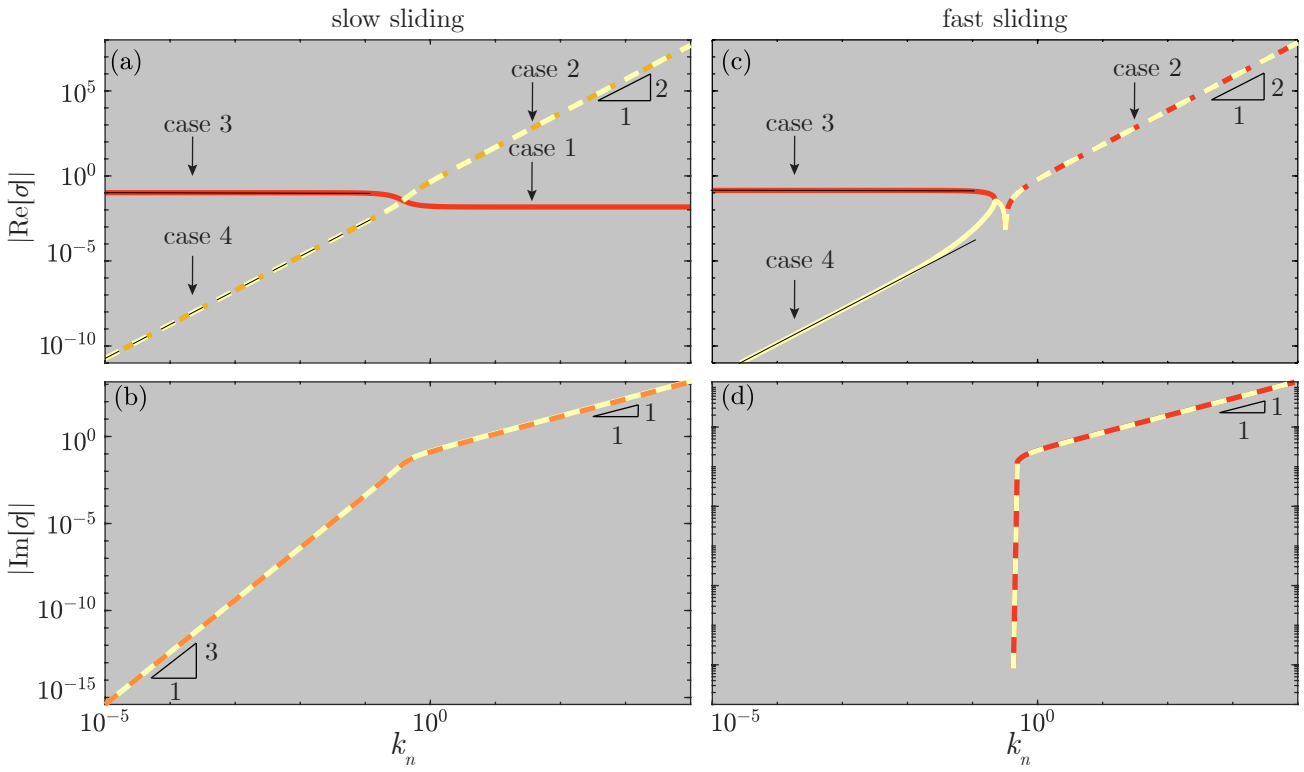

Figure 6: Numerical solution of the dispersion relation (47c) as a function of the wavenumber k. Upper (lower) row displays $|\mathrm{Re}[\sigma]|$, ($|\mathrm{Im}[\sigma]|$), with solid (dashed) line denoting $\mathrm{Re}[\sigma], \mathrm{Im}[\sigma] > 0$ ($\mathrm{Re}[\sigma], \mathrm{Im}[\sigma] < 0$). Columns from left to right illustrate $\bar{U}_b = (0.273, 0.652)$, that is $\gamma = (5, 1)$. Triangular shapes and numbers associated with them denote rise and run of the line best approximating the numerical solution (e.g. a rise of 2 and a run of 1 means $\sigma \sim k^2$ - note that axes are logarithmic). Parameters are $\nu = 1$, $\alpha = 1$, $\Theta_{bed} = -0.5$. The temperature dependent sliding law is $F = \exp(\Theta)$.

where boundedness of temperature in the far field ($\tilde{\mathsf{z}} \to \pm\infty$) is ensured provided $\mathrm{Re}[\sigma^{1/2}] > 0$, while from eqs. (46c- 46d) we get

$$\mathsf{T}_0 = \left[\frac{\bar{\mathsf{h}}^2 k_n^2 \left(3\bar{F} + \bar{\mathsf{h}}\gamma\right) + 3\gamma\sigma}{3_n k \bar{\mathsf{h}} \bar{\mathsf{t}}_b F'}\right] i\hat{\mathsf{h}}_n, \quad \hat{\mathsf{U}}_{b,n} = \left(\frac{\bar{\mathsf{h}}^3 k_n^2 + 3\sigma}{3\bar{\mathsf{h}} k_n}\right) i\hat{\mathsf{h}}_n. \tag{47b}$$

Lastly, the basal energy budget (46g) yields a polynomial expression for the eigenvalue

$$a_0 + a_1 y + a_2 y^2 + a_3 y^3 = 0, \quad \text{with} \quad y = \sigma^{1/2}, \quad \mathrm{Re}[\sigma^{1/2}] > 0, \tag{47c}$$

with coefficients

$$a_0 = \alpha k_n^2 F' \bar{\mathsf{h}}^2 \bar{\mathsf{t}}_b \left(3\bar{\mathsf{U}}_b - \bar{\mathsf{h}}\bar{\mathsf{t}}_b\right), \quad a_1 = 2k_n^2 \bar{\mathsf{h}}^2 \left(\gamma\bar{\mathsf{h}} + 3\bar{F}\right), \quad a_2 = -3\alpha F' \bar{\mathsf{t}}_b^2, \quad a_3 = 6\gamma. \tag{47d}$$

A typical solution is illustrated in figure 6 for slow sliding (panels a-b) and fast sliding (panels c-d); rows illustrate the absolute value of the growth rate (first row) and of the phase speed (second row), with solid (dashed) lines labelling $|\cdot| > 0$ ($|\cdot| < 0$). To validate these results, in §5.1.3 we derive asymptotic approximations of the solution in the short and long wavelength limit, which are reported as thin black lines in figure 6. Key findings from our analysis are that:

1. A solution exists for all wavenumber, but the number of solution changes depending on whether sliding is slow or fast.

2. The system is unconditionally unstable in the long wavelength limit ($k_n \to 0$, red curve labelled *case 3*), while its stability in the short wavelength limit ($k_n \to \infty$) depends on the shearing to sliding ratio: for slow sliding it is unstable (panels a-b, red curve labelled *case 1*), for fast sliding it is unconditionally stable (panels c-d, curves labelled *case 2*).

3. There is no wavelength selection. In the slow sliding regime the system is unstable for all wavelengths from the ice thickness ($k_n \to \infty$) to the ice sheet scale ($k_n \to 0$).

5.1.3 Short wavelength asymptotics

We consider a short wavelength limit, $k_n \to \infty$, and seek a leading order approximation for the solution given by eqs. (46d$_2$, 47a-47c).

Case 1: $\sigma \sim \sigma^{(0)}$

To derive a reduced version of the linearized model (46c-46g) we rescale as

$$\sigma^* = \sigma, \quad \hat{\mathsf{U}}^*_{b,n} = k_n^{-1}\hat{\mathsf{U}}_{b,n}, \quad \hat{\mathsf{h}}^*_n = \hat{\mathsf{h}}_n, \quad \hat{\mathsf{T}}^*_{b,n} = k_n^{-1}\hat{\mathsf{T}}_{b,n}, \quad \frac{\mathrm{d}\hat{\bar{\mathsf{T}}}^*_n}{\mathrm{d}\mathsf{z}} = k_n^{-1}\frac{\mathrm{d}\hat{\bar{\mathsf{T}}}_n}{\mathrm{d}\mathsf{z}}, \quad \hat{\bar{\mathsf{T}}}^*_n = k_n^{-1}\hat{\bar{\mathsf{T}}}_n \tag{48a}$$

Dropping asterisks immediately, and expanding $\sigma \sim \sigma^{(0)} + O(k)$, it is straightforward to show that the solution of the thermal problem, eq. (47a), remains unchanged. The leading order mechanical model is

$$i\bar{\mathsf{h}}\hat{\mathsf{U}}_{b,n} + \frac{\bar{\mathsf{h}}^3}{3}\hat{\mathsf{h}}_n = 0, \tag{48b}$$

$$\hat{\mathsf{U}}_{b,n} = \gamma^{-1}\left(\bar{F}\hat{\mathsf{t}}_{b,n} + \bar{\mathsf{t}}_b F'\mathsf{T}_0\right), \tag{48c}$$

$$\hat{\mathsf{t}}_{b,n} = -i\bar{\mathsf{h}}\hat{\mathsf{h}}_n, \tag{48d}$$

$$-2\mathsf{T}_0\sqrt{\sigma^{(0)}} + \alpha\left(\bar{\mathsf{t}}_b\hat{\mathsf{U}}_{b,n} + \bar{\mathsf{U}}_b\hat{\mathsf{t}}_{b,n}\right) = 0, \tag{48e}$$

which can be solved straightforwardly to yield

$$\sigma^{(0)} = \frac{9\alpha^2\bar{\mathsf{t}}_b^2F'^2\left(-\bar{\mathsf{U}}_b\bar{\mathsf{h}} + \bar{\mathsf{T}}_b\mathsf{h}^2/3\right)^2}{4\bar{\mathsf{h}}\left(3\bar{F} + \bar{\mathsf{h}}\gamma\right)^2}, \quad \hat{\mathsf{U}}_b = \frac{i\bar{\mathsf{h}}^2\hat{\mathsf{h}}_n}{3}, \quad \mathsf{T}_0 = \frac{3\bar{F} + \bar{\mathsf{h}}\gamma}{2F'\bar{\mathsf{T}}_b}i\bar{\mathsf{h}}\hat{\mathsf{h}}_n. \tag{48f}$$

We note that this is a solution provided $-\bar{\mathsf{U}}_b\bar{\mathsf{h}} + \bar{\mathsf{T}}_b\mathsf{h}^2/3 \geq 0$, that is for slow sliding; otherwise we would have $\mathrm{Re}[\sqrt{\sigma^{(0)}}] < 0$, and temperature would be unbounded in the far field. We also note that, after putting $\bar{\mathsf{h}} = 1$ without loss of generality, the expression above is identical to eq. (39b), which holds in the long wavelength limit of the ice thickness scale problem for the slow sliding regime.

Case 2: $\sigma \sim k^2\sigma^{(0)} + O(k)$

To derive a reduced version of the linearized model (46c-46g) we rescale as

$$\sigma^* = k_n^{-2}\sigma, \quad \hat{\mathsf{U}}^*_{b,n} = k^{-1}\hat{\mathsf{U}}_{b,n}, \quad \hat{\mathsf{h}}^*_n = \hat{\mathsf{h}}_n, \quad \hat{\mathsf{T}}^*_{b,n} = k_n^{-1}\hat{\mathsf{T}}_{b,n}, \quad \frac{\mathrm{d}\hat{\bar{\mathsf{T}}}^*_n}{\mathrm{d}\mathsf{z}} = k_n^{-2}\frac{\mathrm{d}\hat{\bar{\mathsf{T}}}_n}{\mathrm{d}\mathsf{z}}, \quad \hat{\bar{\mathsf{T}}}^*_n = k_n^{-1}\hat{\bar{\mathsf{T}}}_n \tag{49a}$$

Dropping asterisks immediately, and expanding $\sigma \sim \sigma^{(0)} + O(k)$, we find that $\hat{\bar{\mathsf{T}}} = 0$ to leading order, while mass conservation (46c) remains unchanged, with sliding velocity and basal shear stress reading

$$\hat{\mathsf{U}}_{b,n} = \gamma^{-1}\bar{F}\hat{\mathsf{t}}_{b,n}, \tag{49b}$$

$$\hat{\mathsf{t}}_{b,n} = -i\bar{\mathsf{h}}\hat{\mathsf{h}}_n. \tag{49c}$$

The solution is straightforward and reads

$$\sigma^{(0)} = -\frac{\left(3\bar{\mathsf{h}}^2\bar{F} + \gamma\bar{\mathsf{h}}^3\right)}{3\gamma}, \tag{49d}$$

which is purely real and always negative. Expanding to $O(k_n)$ we find that this solution has multiplicity 2 and actually gives rise to a stable complex conjugate pair, consistently with the numerical results in figure 6.

5.1.4 Long wavelength asymptotics

We consider a long wavelength limit, $k_n \to 0$, and seek a leading order approximation for the solution given by eqs. ($46d_2$, 47a-47c).

Case 3: $\sigma \sim \sigma^{(0)} + O(k_n)$

We start by taking the limit of $k_n \to 0$ within the model (46c-46g), while keeping all dependent variables strictly of $O(1)$, and expanding $\sigma \sim \sigma^{(0)} + O(k_n)$. We find that the thermal model remains unchanged, with solution (47a), while the leading order mechanical model reads

$$\hat{\mathsf{h}}_n = \hat{\mathsf{t}}_{b,n} = 0, \tag{50a}$$

$$\hat{\mathsf{U}}_{b,n} = \gamma^{-1}\bar{\mathsf{t}}_b F'\mathsf{T}_0, \tag{50b}$$

$$-2\mathsf{T}_0\sqrt{\sigma^{(0)}} + \alpha\bar{\mathsf{t}}_b\hat{\mathsf{U}}_{b,n} = 0, \tag{50c}$$

with solution

$$\sigma^{(0)} = \left(\frac{\alpha F'\bar{\mathsf{T}}_b}{2\gamma}\right)^2, \tag{50d}$$

and perturbed sliding velocity in phase with a prescribed perturbation of basal temperature T_0, according to the sliding law.

The eigenvalue is positive, with $\mathrm{Re}[\sqrt{\sigma}] > 0$, thus we conclude that the system is unconditionally unstable in this limit. We anticipate that a stability analysis of the ice sheet scale model with $\delta \sim \varepsilon^{1/2}$ yields exactly the same result (see §5.2), thus confirming that this unstable mode persists all the way to the ice sheet scale.

Case 4: $\sigma \sim k_n^2\sigma^{(0)} + O(k_n^3)$

To derive a second reduced version of the linearized model (46c-46g) we rescale as

$$\sigma^* = k_n^{-2}\sigma, \quad \hat{\mathsf{U}}^*_{b,n} = k_n^{-1}\hat{\mathsf{U}}_{b,n}, \quad \hat{\mathsf{h}}^*_n = \hat{\mathsf{h}}_n, \quad \hat{\mathsf{T}}^*_{b,n} = k_n^{-1}\hat{\mathsf{T}}_{b,n}, \quad \frac{\mathrm{d}\hat{\bar{\mathsf{T}}}^*_n}{\mathrm{d}\mathsf{z}} = k_n^{-2}\frac{\mathrm{d}\hat{\bar{\mathsf{T}}}_n}{\mathrm{d}\mathsf{z}}, \quad \hat{\bar{\mathsf{T}}}^*_n = k_n^{-1}\hat{\bar{\mathsf{T}}}_n. \tag{51a}$$

Dropping asterisks immediately, it's straightforward to show that the heat equation admits a constant solution $\hat{\bar{\mathsf{T}}} = T_0$; mass conservation and the sliding law, eqs. (46c,46d) remain unchanged, while the leading order basal energy budget reads

$$\bar{\mathsf{U}}_b \hat{\mathsf{t}}_{b,n} + \bar{\mathsf{T}}_b \hat{\mathsf{U}}_{b,n} = 0. \tag{51b}$$

The solution to this version of the linearized problem is

$$\sigma^{(0)} = \bar{\mathsf{h}} \frac{\left(\bar{\mathsf{h}}\bar{\mathsf{U}}_b - \bar{\mathsf{h}}^2 \bar{\mathsf{T}}_b/3\right)}{\bar{\mathsf{T}}_b}, \quad \hat{\mathsf{U}}_{b,n} = \frac{i\bar{\mathsf{h}}\bar{\mathsf{U}}_b \hat{\mathsf{h}}_n}{\bar{\mathsf{T}}_b}, \quad \mathsf{T}_0 = \frac{i\bar{\mathsf{h}}\hat{\mathsf{h}}_n \left(\gamma \bar{\mathsf{U}}_b + \bar{F}\bar{\mathsf{T}}_b\right)}{F' \bar{\mathsf{T}}_b^2}, \tag{51c}$$

where the growth rate is positive ($\sigma^{(0)} > 0$) if $\bar{\mathsf{h}}\bar{\mathsf{U}}_b - \bar{\mathsf{h}}^2 \bar{\mathsf{T}}_b/3 > 0$, which identifies the fast sliding regime, and negative otherwise. We note that this version of the reduced model corresponds to the short wavelength limit of the shallow slab with subtemperate sliding, with growth rate given by eq. (9e).

5.2 Stability of the ice sheet scale model

Here we analyze the stability properties of the ice sheet scale model (26). Recalling that the ice thickness is independent of the fast time scale to leading oder, and so is the basal shear stress, we expand dependent variables as

$$h^{(0)} = \bar{h}, \quad {u_b}^{(0)} = \bar{u_b} + \beta u_b', \quad {\tau_b}^{(0)} = \bar{\tau_b}, \quad \tilde{T}^{(0)} = \bar{\tilde{T}} + \beta \tilde{T}', \quad \beta \ll 1 \tag{52a}$$

where barred quantities are independent of x, τ. Assuming as usual a periodic domain with length L, we Fourier-transform perturbed variables in x as

$$\hat{g}_n = \frac{1}{L} \int_0^L g' \exp\left(-ik_n x\right) \mathrm{d}x, \quad k_n = \frac{2\pi n}{L} \tag{52b}$$

and we also assume separation of variable, so that $\partial \hat{g}_n / \partial \tau = \sigma \hat{g}_n$. Substituting into the governing equations and linearizing, we find to $O(\beta)$

$$\sigma \hat{\tilde{T}}_n - \frac{\mathrm{d}^2 \hat{\tilde{T}}_n}{\mathrm{d}\tilde{z}^2} = 0, \quad \text{for} \quad -\infty < \tilde{z} < +\infty, \tag{52c}$$

with boundary conditions

$$\frac{\mathrm{d}\hat{\tilde{T}}_n}{\mathrm{d}\tilde{z}} \to 0 \qquad \text{as} \quad \tilde{z} \to \pm\infty, \tag{52d}$$

$$\left[\frac{\mathrm{d}\hat{\tilde{T}}_n}{\mathrm{d}\tilde{z}}\right]_-^+ + \alpha \bar{\tau_b} \hat{u}_{b,n} = 0 \qquad \text{on} \quad \tilde{z} = 0. \tag{52e}$$

and sliding law

$$\hat{u}_{b,n} = \gamma^{-1} \bar{\tau_b} F' \hat{\tilde{T}}_n|_{\tilde{z}=0}, \tag{52f}$$

with $F' = \mathrm{d}F/\mathrm{d}\tilde{T}|_{\bar{\tilde{T}}}$ evaluated on $\tilde{z} = 0$.

The linear problem above can be solved straightforwardly: the heat equation has solution

$$\hat{\tilde{T}}_n = \begin{cases} T_0 \exp\left(-\tilde{z}\sigma^{1/2}\right) & \text{for } \tilde{z} > 0 \\ T_0 \exp\left(\tilde{z}\sigma^{1/2}\right) & \text{for } \tilde{z} < 0 \end{cases} \tag{52g}$$

where boundedness of temperature in the far field ($\tilde{z} \to \pm\infty$) is ensured provided $\mathrm{Re}[\sigma^{1/2}] > 0$. The basal energy budget and the sliding law then yield the eigenvalue

$$\sigma = \left(\frac{\alpha F' \bar{\tau}_b}{2\gamma} \right)^2, \tag{52h}$$

while the perturbed sliding velocity can be computed from eq. (52f) for any prescribed basal temperature perturbation T_0.

We conclude by noting that i) the eigenvalue is positive with $\mathrm{Re}[\sigma^{1/2}] > 0$, thus the system is unconditionally unstable; ii) the eigenvalue is independent of the wavenumber, so there is no cut-off and all wavelengths in the ice sheet scale model are unstable.

6 The discrete ice thickness scale subtemperate slab with $\delta \sim \varepsilon^{1/2}$

In this section we formulate a discrete versionof the ice thickness scale model with subtemperate sliding and finite δ described in §2.3.1.

6.1 Model reformulation

To facilitate the solution of the mechanical model, we reformulate the Stokes problem (21) in terms of streamfunction ψ defined as

$$U^{(0)} = \frac{\partial \psi}{\partial Z}, \quad W^{(0)} = -\frac{\partial \psi}{\partial X}, \tag{53a}$$

and vorticity

$$\omega = \frac{\partial^2 \psi}{\partial X^2} + \frac{\partial^2 \psi}{\partial Z^2}, \tag{53b}$$

and apply the rescalings (31). Then, following Batchelor [7] and dropping asterisks for simplicity, the Stokes problem can be rewritten in terms of vorticity and streamfunction as

$$\nabla^2 \psi = \omega, \tag{54a}$$

$$\nabla^2 \omega = 0, \tag{54b}$$

on $0 < Z < 1$, $0 < X < L$, where L is the length of the subtemperate slab. Boundary conditions at the surface and at the base are

$$\psi = \omega = 0 \qquad \text{on} \quad Z = 1, \tag{54c}$$

$$\psi = 0 \qquad \text{on} \quad Z = 0, \tag{54d}$$

$$\omega = \frac{\gamma}{F({\Theta_b}^{(1)})} \frac{\partial \psi}{\partial Z} \qquad \text{on} \quad Z = 0, \tag{54e}$$

where $F(\theta) = \exp(\Theta)$, while we apply periodic boundary conditions on vertical domain boundaries,

$$\left[\frac{\partial \psi}{\partial X} \right]_-^+ = \left[\frac{\partial \omega}{\partial X} \right]_-^+ = [\psi]_-^+ = [\omega]_-^+ = 0 \quad \text{on} \quad X = 0, L. \tag{54f}$$

The leading order model for the thermal boundary layer (24) with the outer problem (21k) remain unchanged under rescaling, while periodicity of the domain implies

$$\left[\frac{\partial \mathcal{Q}^{(0)}}{\partial X} \right]_-^+ = \left[\frac{\partial \tilde{\Theta}^{(0)}}{\partial \tilde{X}} \right]_-^+ = 0 \quad \text{on} \quad X, \tilde{X} = 0, L. \tag{55}$$

6.2 Discretization

Model variables are stream function, ψ, vorticity ω, boundary layer temperature $\tilde{\Theta}$, and outer heat flux $\mathcal{Q}$, where we have dropped superscripts for simplicity. We discretize our model using finite volumes and a backward Euler's method; we label time steps with the superscript i, which we take to assume only integer values, and we will use a constant time step $\Delta\tau$ throughout.

For the mechanical problem the computational domain is the strip $0 < X < L$, and $0 < Z < 1$, where we define a regular, two-dimensional, rectilinear grid locally refined near the ice-bed interface (in the vertical direction). The grid has N_h grid points in the horizontal and N_v grid points in the vertical, with ψ and ω defined at cell centres. The ice-bed contact, $Z = 0$, and the ice surface $Z = 1$ are cell boundaries, and so are inflow and outflow boundaries, located at $X = 0, L$.

We label $\psi-$grid points by indices $\alpha = 1, 2, \ldots, N_h$ and $\beta = 1, 2, \ldots, N_v$, so that $\alpha = 1/2, N_h + 1/2$ are the inflow and outflow boundaries, respectively, while $\beta = 1/2, N_v^i + 1/2$ are the ice-bed interface and the ice surface. Lastly, we introduce the indexes $1 \le j \le N_h$, $1 \le k \le N_v^i$, where the indices j, k are restricted to integer values; the spacing between $\psi-$grid points is ΔX, ΔZ_k, with the position of grid points given by

$$Z_\beta = \left[\left(\beta - \frac{1}{2}\right)\frac{1}{N_v^i}\right]^m, \quad X_\alpha = \left(\alpha - \frac{1}{2}\right)\frac{L_h}{N_h}, \tag{56a}$$

where $m \ge 1$, and $m = 1$ denotes an evenly spaced grid.

For the thermal problem, we treat inner and outer problems separately. For the inner temperature field, our computational domain is the strip $0 < X < L$, and $-L_v < Z < L_v$ (with $L_v > 1$), where we define a regular, two-dimensional, rectilinear grid locally refined near the ice-bed interface (in the vertical direction). The grid has N_h grid points in the horizontal and $N_v^b + N_v^i + 1$ grid points in the vertical, with $\tilde{\Theta}$ defined at cell centres. Note that the $\tilde{\Theta}-$grid is horizontally staggered with respect to the $\psi-$grid, so that $\tilde{\Theta}-$nodes are located on ψ cell boundaries. Accordingly, the ice-bed contact, and inflow and outflow boundaries.

We label $\Theta-$grid points by indices $\alpha = 1/2, 3/2, \ldots, N_h - 1/2$ and $\gamma = -N_v^b, -N_v^b + 1, \ldots, N_v^i$, so that $\alpha = 1/2, N_h - 1/2$ are the inflow and outflow boundaries, respectively, and $\gamma = 1/2, N_v^i + 1/2$ are the ice-bed interface and the top of the boundary layer. The spacing between $\tilde{\Theta}-$grid points is $\Delta\tilde{X} = \Delta X$, $\Delta\tilde{Z}_l$, where we take the integer indices $1 \le j \le N_h$, $1 \le l \le N_v^i + N_v^b + 1$. Then the position of grid points is given by

$$Z_\gamma = \begin{cases} \left[\left(\gamma - \frac{1}{2}\right)\frac{L_v}{N_v^i}\right]^m & \text{for} \quad 1 \le \gamma \le N_v^i + 1 \\ -\left|\left(\gamma - \frac{1}{2}\right)\frac{L_v}{N_v^b}\right|^m & \text{for} \quad -N_v^b \le \gamma < 1 \end{cases}, \quad X_\alpha = \left(\alpha - \frac{1}{2}\right)\frac{L_h}{N_h}. \tag{56b}$$

Lastly, for the thermal outer problem, we restrict ourselves to a one-dimensional grid co-located with the the $\tilde{\Theta}-$grid. Horizontal grid spacing will be ΔX, and grid points will be labelled by $\alpha = 1/2, 3/2, \ldots, N_h - 1/2$.

6.2.1 Mechanical problem

For the biharmonic problem (54a-54b) we use a second-order centered scheme both in the horizontal and in the vertical, so in discrete form we get

$$\frac{\psi^i_{j+1,k} - 2\psi^i_{j,k} + \psi^i_{j-1,k}}{\Delta X^2} + \frac{1}{\Delta Z_k}\left[\frac{2\left(\psi^i_{j,k+1} - \psi^i_{j,k}\right)}{\Delta Z_{k+1} + \Delta Z_k} - \frac{2\left(\psi^i_{j,k} - \psi^i_{j,k-1}\right)}{\Delta Z_k + \Delta Z_{k-1}}\right] = \omega_{j,k}, \tag{57a}$$

$$\frac{\omega^i_{j+1,k} - 2\omega^i_{j,k} + \omega^i_{j-1,k}}{\Delta X^2} + \frac{1}{\Delta Z_k}\left[\frac{2\left(\omega^i_{j,k+1} - \omega^i_{j,k}\right)}{\Delta Z_{k+1} + \Delta Z_k} - \frac{2\left(\omega^i_{j,k} - \omega^i_{j,k-1}\right)}{\Delta Z_k + \Delta Z_{k-1}}\right] = 0. \tag{57b}$$

Regarding boundary condition, for $j = 1, N_h$ the equations above require ω and ψ at the fictitious grid points $\alpha = j - 1 = 0$ and $\alpha = j + 1 = N_h + 1$. Given that our domain is periodic in X, we simply put

$$\psi^i_{0,k} = \psi^i_{N_h,k}, \quad \omega^i_{0,k} = \omega^i_{N_h,k}, \tag{57c}$$

which, along with the finite volume discretization and the centered scheme for ψ and ω, automatically ensure that both the normal flux and the two variables remains continuous. At the ice surface, $\beta = k + 1/2 = N_v + 1/2$, boundary conditions (54c) apply, so we put

$$\begin{aligned}\frac{2\left(\psi^i_{j,k+1} - \psi^i_{j,k}\right)}{\Delta Z_{k+1} + \Delta Z_k} =& 2\frac{\left(\Delta Z^2_{k-1} + 4\Delta Z_k\Delta Z_{k-1} + 3\Delta Z^2_k\right)}{\Delta Z_k(\Delta Z_k + \Delta Z_{k-1})(2\Delta Z_k + \Delta Z_{k-1})} \\ &+ 2\frac{\Delta Z^2_k\psi^i_{j,k-1} - (\Delta Z_{k-1} + 2\Delta Z_k)^2\psi^i_{j,k}}{\Delta Z_k(\Delta Z_k + \Delta Z_{k-1})(2\Delta Z_k + \Delta Z_{k-1})} \quad \text{for} \quad k = N_v \end{aligned} \tag{57d}$$

$$\frac{2\left(\omega^i_{j,k+1} - \omega^i_{j,k}\right)}{\Delta Z_{k+1} + \Delta Z_k} = 2\frac{\Delta Z^2_k\omega^i_{j,k-1} - (\Delta Z_{k-1} + 2\Delta Z_k)^2\omega^i_{j,k}}{\Delta Z_k(\Delta Z_k + \Delta Z_{k-1})(2\Delta Z_k + \Delta Z_{k-1})} \quad \text{for} \quad k = N_v, \tag{57e}$$

where we have used a second-order accurate polynomial extrapolation on the boundary to compute fluxes there. Similarly, to satisfy the boundary conditions (54d-54e) at the bed, $\beta = k - 1/2 = 1/2$, we put

$$\frac{2\left(\psi^i_{j,k} - \psi^i_{j,k-1}\right)}{\Delta Z_k + \Delta Z_{k-1}} = -2\frac{\Delta Z^2_k\psi^i_{j,k+1} - (\Delta Z_{k+1} + 2\Delta Z_k)^2\psi^i_{j,k}}{\Delta Z_k(\Delta Z_k + \Delta Z_{k+1})(2\Delta Z_k + \Delta Z_{k+1})} \quad \text{for} \quad k = 1, \tag{57f}$$

$$\begin{aligned}\frac{2\left(\omega^i_{j,k} - \omega^i_{j,k-1}\right)}{\Delta Z_k + \Delta Z_{k-1}} =& -2\frac{\left(\Delta Z^2_{k+1} + 4\Delta Z_k\Delta Z_{k+1} + 3\Delta Z^2_k\right)\omega^i_{j,k-1/2}}{\Delta Z_k(\Delta Z_k + \Delta Z_{k+1})(2\Delta Z_k + \Delta Z_{k+1})} \\ &- 2\frac{\Delta Z^2_k\omega^i_{j,k+1} - (\Delta Z_{k+1} + 2\Delta Z_k)^2\omega^i_{j,k}}{\Delta Z_k(\Delta Z_k + \Delta Z_{k+1})(2\Delta Z_k + \Delta Z_{k+1})} \quad \text{for} \quad k = 1, \end{aligned} \tag{57g}$$

with

$$\omega^i_{j,1/2} = \frac{\gamma}{F(\Theta^i_{bed,j})}\frac{2\left(\psi^i_{j,k} - \psi^i_{j,k-1}\right)}{\Delta Z_k + \Delta Z_{k-1}}, \quad \text{for} \quad k = 1, \tag{57h}$$

where $\Theta^i_{bed,j} = (\Theta^i_{bed,j+1/2} + \Theta^i_{bed,j-1/2})/2$ is constrained by the basal energy budget of the bed (24a). For simplicity, we treat this along with the thermal problem in the next section.

6.2.2 Thermal problem

Next we look at the thermal problem in the boundary layer near the bed. Energy conservation is discretized with a second-order centered scheme for both advective and diffusive fluxes; for the ice,

$1 \le j \le N_h$ and $N_v^b + 1 \le l \le N_v^i + N_v^b + 1$, we have

$$\begin{aligned}\frac{\tilde{\Theta}^i_{j-1/2,l} - \tilde{\Theta}^{i-1}_{j-1/2,l}}{\Delta\tau} + \frac{U^i_j\left(\tilde{\Theta}^i_{j+1/2,l} + \tilde{\Theta}^i_{j-1/2,l}\right) - U^i_{j-1}\left(\tilde{\Theta}_{j-1/2,l} + \tilde{\Theta}^i_{j-3/2,l}\right)}{2\Delta\tilde{X}} + \\ \frac{1}{\Delta\tilde{Z}_l}\left[W^i_{j-1/2,l+1/2}\frac{\tilde{\Theta}^i_{j-1/2,l+1}\Delta\tilde{Z}_l + \tilde{\Theta}^i_{j-1/2,l}\Delta\tilde{Z}_{l+1}}{\Delta\tilde{Z}_{l+1} + \Delta\tilde{Z}_l} - \right. \\ \left. W^i_{j-1/2,l-1/2}\frac{\tilde{\Theta}^i_{j-1/2,l}\Delta\tilde{Z}_{l-1} + \tilde{\Theta}^i_{j-1/2,l-1}\Delta\tilde{Z}_l}{\Delta\tilde{Z}_l + \Delta\tilde{Z}_{l-1}}\right] - \\ \frac{1}{\Delta\tilde{Z}_l}\left[\frac{2\left(\tilde{\Theta}^i_{j-1/2,l+1} - \tilde{\Theta}^i_{j-1/2,l}\right)}{\Delta\tilde{Z}_{l+1} + \Delta\tilde{Z}_l} - \frac{2\left(\tilde{\Theta}^i_{j-1/2,l} - \tilde{\Theta}^i_{j-1/2,l-1}\right)}{\Delta\tilde{Z}_l + \Delta\tilde{Z}_{l-1}}\right] = 0,\end{aligned} \tag{58a}$$

while for the bed, that is $1 \le j \le N_h$ and $1 \le l \le N_v^b$, we have

$$\frac{\tilde{\Theta}^i_{j-1/2,l} - \tilde{\Theta}^{i-1}_{j-1/2,l}}{\Delta\tau} - \frac{1}{\Delta\tilde{Z}_l}\left[\frac{2\left(\tilde{\Theta}^i_{j-1/2,l+1} - \tilde{\Theta}^i_{j-1/2,l}\right)}{\Delta\tilde{Z}_{l+1} + \Delta\tilde{Z}_l} - \frac{2\left(\tilde{\Theta}^i_{j-1/2,l} - \tilde{\Theta}^i_{j-1/2,l-1}\right)}{\Delta\tilde{Z}_l + \Delta\tilde{Z}_{l-1}}\right] = 0. \tag{58b}$$

Recalling the definitions (23b), horizontal and vertical velocities are computed in terms of stream function and vorticity as

$$U^i_j = \frac{F(\tilde{\Theta}^i_{j,1/2})}{\gamma}\omega^i_{j,1/2}, \tag{58c}$$

$$W^i_{j-1/2,l+1/2} = \frac{U_j - U_{j-1}}{\Delta\tilde{X}}\tilde{Z}_{l+1/2}. \tag{58d}$$

Regarding boundary conditions, we start from the top of the boundary layer, $l = N_v^b + N_v^i + 1$. Here the matching condition ($24e_1$) couples the boundary layer problem to the advection-only outer problem for $\mathcal{Q}^i_{j-1/2}$ through

$$-\frac{2\left(\tilde{\Theta}^i_{j-1/2,l+1} - \tilde{\Theta}^i_{j-1/2,l}\right)}{\Delta\tilde{Z}_{l+1} + \Delta\tilde{Z}_l} = \mathcal{Q}^i_{j-1/2} \quad \text{for} \quad l = N_v^b + N_v^i + 1, \tag{58e}$$

which we then use to compute temperature at the fictitious grid point $l = N_v^b + N_v^i + 2$, as required by the advective heat flux, through linear extrapolation,

$$\tilde{\Theta}^i_{j-1/2,N_v^b+N_v^i+2} = \tilde{\Theta}^i_{j-1/2,N_v^b+N_v^i+1} + \mathcal{Q}^i_{j-1/2}\Delta\tilde{Z}_{N_v^b+N_v^i+1}. \tag{58f}$$

Note that this is consistent with the structure of the underlying continuum problem, which is such that the temperature profile should become linear at sufficient distance from the bed. Numerical results show that a boundary layer height $L_v = 3$ is typically sufficient to recover a linear temperature profile.

The outer heat flux $\mathcal{Q}^i_{j-1/2}$ evolves according to the $Q-$equation, which in discrete form reads

$$\frac{\mathcal{Q}^i_{j-1/2} - \mathcal{Q}^{i-1}_{j-1/2}}{\Delta\tau} + \frac{U^i_j\left(\mathcal{Q}^i_{j+1/2} + \mathcal{Q}^i_{j-1/2}\right) - U^i_{j-1}\left(\mathcal{Q}^i_{j-1/2} + \mathcal{Q}^i_{j-3/2}\right)}{2\Delta X} - \mathcal{Q}^i_{j-1/2}\frac{U^i_j - U^i_{j-1}}{\Delta X} = 0, \tag{58g}$$

with periodic boundary conditions

$$\mathcal{Q}^i_{-1/2} = \mathcal{Q}^i_{N_h-1/2}. \tag{58h}$$

At the bed, $\gamma = l - N_v^b - 1/2 = 1/2$, continuity of basal temperature is enforced through one-sided approximations of the vertical heat fluxes,

$$\begin{aligned} \frac{2\left(\tilde{\Theta}^i_{j-1/2,l+1} - \tilde{\Theta}^i_{j-1/2,l}\right)}{\Delta\tilde{Z}_{l+1} + \Delta\tilde{Z}_l} &= \frac{\Theta^i_{bed,j-1/2} - \tilde{\Theta}^i_{j-1/2,l}}{\Delta\tilde{Z}_l} \quad \text{for} \quad l = N_v^b, \\ \frac{2\left(\tilde{\Theta}^i_{j-1/2,l} - \tilde{\Theta}^i_{j-1/2,l-1}\right)}{\Delta\tilde{Z}_l + \Delta\tilde{Z}_{l-1}} &= \frac{\tilde{\Theta}^i_{j-1/2,l} - \Theta^i_{bed,j-1/2}}{\Delta\tilde{Z}_l} \quad \text{for} \quad l = N_v^b + 1, \end{aligned} \tag{58i}$$

where basal temperature $\Theta_{bed,j-1/2}$ is constrained by the basal energy budget

$$\frac{\tilde{\Theta}^i_{j-1/2,N_v^b+1} - \Theta^i_{bed,j-1/2}}{\Delta\tilde{Z}_{N_v^b+1}} - \frac{\Theta^i_{bed,j-1/2} - \tilde{\Theta}^i_{j-1/2,N_v^b}}{\Delta\tilde{Z}_{N_v^b}} + \alpha\left(\frac{U^i_j + U^i_{j-1}}{2}\right)\left(\frac{\omega^i_{j,1/2} + \omega^i_{j-1,1/2}}{2}\right) = 0 \tag{58j}$$

and the basal shear stress $\omega^i_{j-1,1/2}$ is given by eq. (57h).

A Supplementary Figures

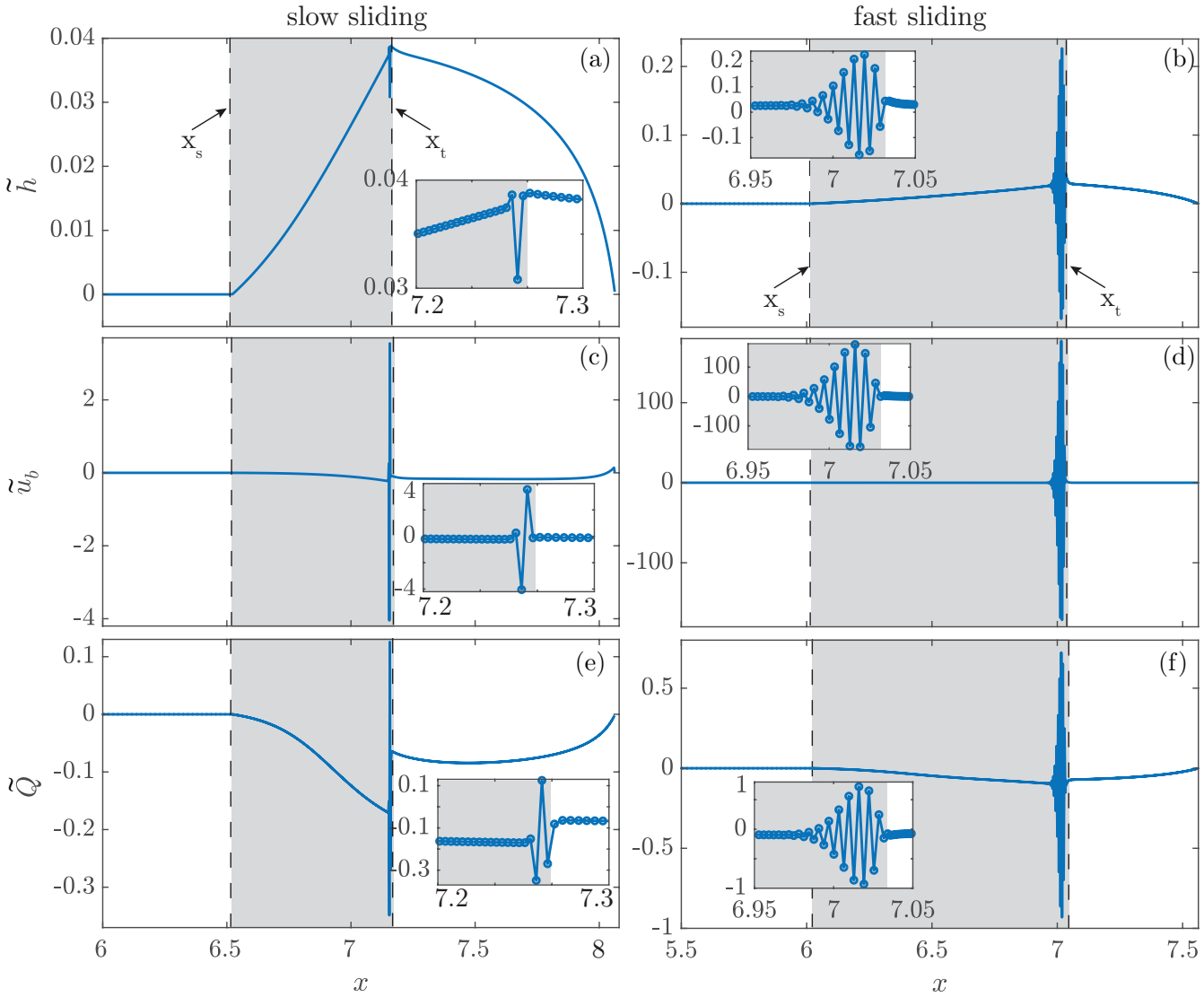

Figure 7: Results from the numerical stability analysis of the ice sheet scale model with subtemperate sliding presented in §(3(b)) of the main text. Along rows: ice thickness, sliding velocity, and basal heat flux perturbation associated with the fastest growing eigenvalue for $\gamma = 1.7$ (left column) and $\gamma = 0.7$ (right column). The subtemperate region is shaded, and insets show a zoom near the subtemperate-temperate boundary. Parameters are $\alpha = 0.4$, $\nu = 0.5$, $Pe = 7.5$, $T_S = -1$, $q_0 = 5$. The number of computational grid points is $N_h = 320$, $N_T = 320 \times 320$ for each subdomain. Note that the divide (not shown) is located at $x = 0$.

References

[1] A.C. Fowler and D.A. Larson. On the flow of polythermal glaciers. i. Model and preliminary analysis. *Proc. R. Soc. Lond. A*, 363:217–242, 1978.

[2] L.W. Morland and I.R. Johnson. The steady motion of ice sheets. *J. Glaciol.*, 25:229–246, 1980.

[3] C. Schoof. Marine ice-sheet dynamics. Part 1. The case of rapid sliding. *J. Fluid Mech.*, 573: 27–55, 2007.

[4] A. C. Fowler. Sub-temperate basal sliding. *J. Glaciol.*, 32(110):3–5, 1986.

[5] R.L. Shreve. Glacier sliding at subfreezing temperatures. *J. Glaciol.*, 30(106):341–347, 1984.

[6] A.C. Fowler. Modelling the flow of glaciers and ice sheets. In *Continuum Mechanics and Applications in Geophysics and the Environment*, pages 201–221. Springer, Berlin, 2001.

[7] G. K. Batchelor. *An Introduction to Fluid Dynamics*. Cambridge University Press, 2000.